arXiv:astro-ph/0212226 v2 16 Jan 2003

Hot Stars: Old-Fashioned or Trendy?

A. W. A. Pauldrach

Institut für Astronomie und Astrophysik der Universität München
Scheinerstraße 1, 81679 München, Germany
UH10107@usm.uni-muenchen.de,
http://www.usm.uni-muenchen.de/people/adi/adi.html

Abstract

Spectroscopic analyses with the intention of the interpretation of the UV-spectra of the brightest stars as individuals – supernovae – or as components of star-forming regions – massive O stars – provide a powerful tool with great astrophysical potential for the determination of extragalactic distances and of the chemical composition of star-forming galaxies even at high redshifts.

The perspectives of already initiated work with the new generation of tools for quantitative UV-spectroscopy of Hot Stars that have been developed during the last two decades are presented and the status of the continuing effort to construct corresponding models for Hot Star atmospheres is reviewed.

Since the physics of the atmospheres of Hot Stars are strongly affected by velocity expansion dominating the spectra at all wavelength ranges, hydrodynamic model atmospheres for O-type stars and explosion models for Supernovae of Type Ia are necessary as basis for the synthesis and analysis of the spectra. It is shown that stellar parameters, abundances, and stellar wind properties can be determined by the methods of spectral diagnostics already developed. Additionally, it will be demonstrated that models and synthetic spectra of Type Ia Supernovae of required quality are already available. These will make it possible to tackle the question of whether Supernovae Ia are standard candles in a cosmological sense, confirming or disproving that the current SN-luminosity distances indicate accelerated expansion of the universe.

In detail we discuss applications of the diagnostic techniques by example of two of the most luminous O supergiants in the Galaxy and a standard Supernova of Type Ia. Furthermore, it is demonstrated that the spectral energy distributions provided by state-of-the-art models of massive O stars lead to considerably better agreement with observations if used for the analysis of H II regions. Thus, an excellent way of determining extragalactic abundances and population histories is offered.

Moreover, the importance of Hot Stars in a broad astrophysical context will be discussed. As they dominate the physical conditions of their local environments and the life cycle of gas and dust of their host galaxies, special emphasis will be given to the corresponding diagnostic perspectives. Beyond that, the relevance of Hot Stars to cosmological issues will be considered.

1 Introduction

It is well known that Hot Stars are not a single group of objects but comprise sub-groups of objects in different parts of the HR diagram and at different evolutionary stages. The most important sub-groups are massive O/B stars, Central Stars of Planetary Nebulae, and Supernovae of Type Ia and II. All these sub-groups have in common that they are characterized by high radiation energy densities and expanding atmospheres, and due to this the state of the outermost parts of these objects is characterized by non-equilibrium thermodynamics. In order to cover the best-known fundamental stages of the evolution of Hot Stars in sufficient depth this review will be restricted to the discussion of O stars and Supernovae of Type Ia; we will not discuss objects like Wolf-Rayet stars, Luminous Blue Variables, Be-stars, Supernovae of Type II, and others. Furthermore, Hot Stars play an important role in a broad astrophysical context. This implies that a complete review covering all aspects in theory and observation is not only impossible, but also beyond the scope of this review. Thus, this review will focus on a special part of the overall topic with the intent to concentrate on just one subject; the subject chosen is UV spectral diagnostics. It will be shown, however, that this subject has important implications for astrophysical topics which are presently regarded as being "trendy".

But first of all we have to clarify what UV spectral diagnostics means. This is best illustrated by the really old-fashioned (1977, Morton and Underhill) UV spectrum of one of the brightest massive O stars, the O4 I(f) supergiant ζ Puppis. As can be seen in Figure 1, expanding atmospheres have a pronounced effect on the emergent spectra of hot stars – especially in the UV-part. The signatures of outflow are clearly recognized by the blue-shifted absorption and red-shifted emission in the form of the well-known P Cygni profiles. It is quite obvious that these kind of spectra contain information not only about stellar and wind parameters, but also about abundances. Thus, in principle, all fundamental parameters of a hot star can be deduced from a comparison of observed and synthetic spectra.

Although spectra of the quality shown in Figure 1 have been available for more than 25 years, most of the work done to date has concentrated on qualitative results and arguments. In view of the effort put into the development of modern – state-of-the-art – instruments, it is certainly not sufficient to restrict the analyses to simple line identifications and qualitative estimates of the physical properties. The primary objective must be to extract the complete physical stellar information from these spectra. Such diagnostic issues principally have been made possible by the superb quality and spectral resolution of the spectra available.

For this objective, the key is to produce realistic synthetic UV spectra for Hot Stars. Such powerful tools, however, are still in development and not yet widely used. They offer the opportunity to determine the stellar parameters, the abundances of the light elements – He, C, N, O, Si – and of the heavy elements like Fe and Ni, quantitatively, as is indicated not only by IUE, but also more recent HST, ORFEUS, and FUSE observations of hot stars in the Galaxy and Local Group galaxies. All these observations show that the spectra in the UV spectral range are dominated by a dense forest of slightly wind-affected pseudo-photospheric metal absorption lines

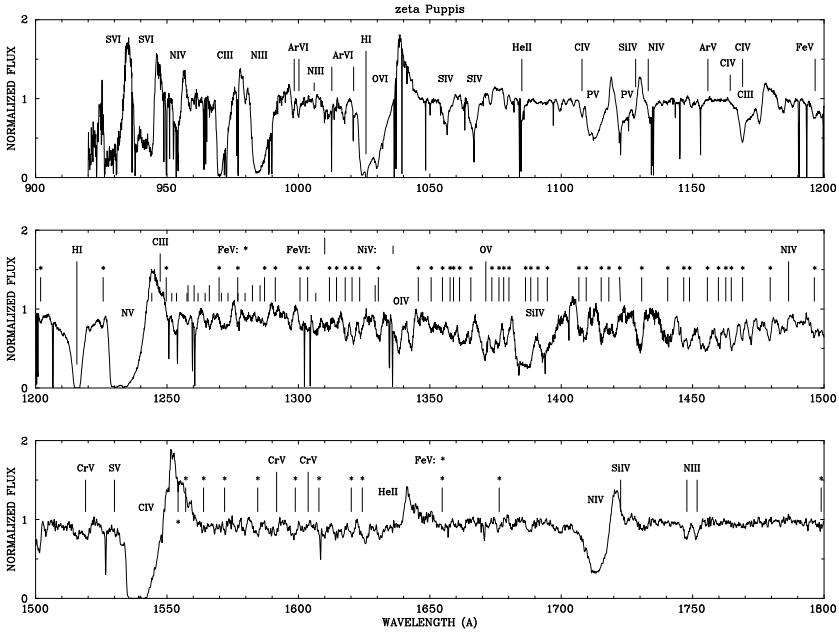

Figure 1: Merged spectrum of Copernicus and IUE UV high-resolution observations of the O4 I(f) supergiant ζ Puppis (900–1500 Å: Morton and Underhill 1977; 1500–1800 Å: Walborn et al. 1985). The most important wind lines of the light elements are identified and marked. Also marked are the large number of wind-contaminated lines of the iron group elements (e.g., Fe V) which are especially present between 1250 and 1500 Å. (Figure from Pauldrach et al. 1994b).

overlaid by broad P Cygni line profiles of strong, mostly resonance lines, formed in different parts of the expanding atmosphere. Thus, the obvious objective is to investigate the importance of these lines with respect to the structure of the expanding atmospheres that are characterized by the strength and the velocity of the outflow, and through which the shape of the spectral lines is mainly determined. Over the last 30 years it turned out that the achievement of this objective, which will also be the primary aim of this paper to review, remains a difficult task.

Before we discuss in detail the status quo of the diagnostic tool required (Section 6), we will first examine whether such a tool has been made obsolete by the general development in astrophysics or whether it is still relevant to current astronomical research.

For this purpose we first discuss the diagnostic perspectives of galaxies with pronounced current star formation. Due to the impact of massive stars on their environment the physics underlying the spectral appearance of starburst galaxies are rooted in the atmospheric expansion of massive O stars which dominate the UV wavelength range in star-forming galaxies. Therefore, the UV-spectral features of massive O stars can be used as tracers of age and chemical composition of starburst galaxies even at high redshift (Section 2).

With respect to the present cosmological question of the reionization of the universe – which appeared to have happened at a redshift of about $z \sim 6$ – the ionization efficiency of a top-heavy Initial Mass Function for the first generations of stars is discussed (Section 3).

Starting from the impact of massive stars on their environment it is demonstrated that the spectral energy distributions provided by state-of-the-art models of massive O stars lead to considerable improvements if used for the analysis of H II regions. Thus, the corresponding methods for determining extragalactic abundances and population histories are promising (Section 4).

Regarding diagnostic issues, the role of Supernovae of Type Ia as distance indicators is discussed. The context of this discussion concerns the current and rather surprising surprising result that distant SNe Ia appear fainter than standard candles in an empty Friedmann model of the universe (Section 5).

Finally, we discuss applications of the diagnostic techniques by example of two of the most luminous O supergiants in the Galaxy; additionally, basic steps towards realistic synthetic spectra for Supernovae of Type Ia are presented (Section 7).

2 The impact of massive stars on their Environment – UV Spectral Analysis of Starburst Galaxies

The impact of massive stars on their environment in the present phase of the universe is of major importance for the evolution of most galaxies. Although rare by number, massive stars dominate the life cycle of gas and dust in star forming regions and are responsible for the chemical enrichment of the ISM, which in turn has a significant impact on the chemical evolution of the host galaxy. This is mainly due to the short lifetimes of massive stars, which favours the recycling of heavy elements in an extremely efficient way. Furthermore, the large amount of momentum and energy input of these objects into the ISM controls the dynamical evolution of the ISM. This takes place in an extreme way, because massive stars mostly group in young clusters, producing void regions around themselves and wind- and supernova-blown superbubbles around the clusters. These superbubbles are ideal places for further star formation, as numerous Hubble Space Telescope images show. Investigation of these superbubbles will finally yield the required information to understand the various processes leading to continuous star formation regions (cf. Oey and Massey 1995). The creation of superbubbles is also responsible for the phenomenon of galactic energetic outflows observed in starbursts (Kunth et al. 1998) and starburst galaxies even at high redshift (Pettini et al. 1998). It is thus not surprising that spectroscopic studies of galaxies with pronounced current star formation reveal the specific spectral signatures of massive stars, demonstrating in this way that the underlying physics for the spectral appearance of starburst galaxies is not only rooted in the atmospheric expansion of massive O stars, but also dominated by these objects (cf. Figure 2 from Steidel et al. 1996, for star-forming galaxies at high redshift see also Pettini et al. 2000, and for UV line spectra of local star-forming galaxies see Conti et al. 1996; note that the similarity of the spectra at none/low and high redshifts suggests a similar stellar content).

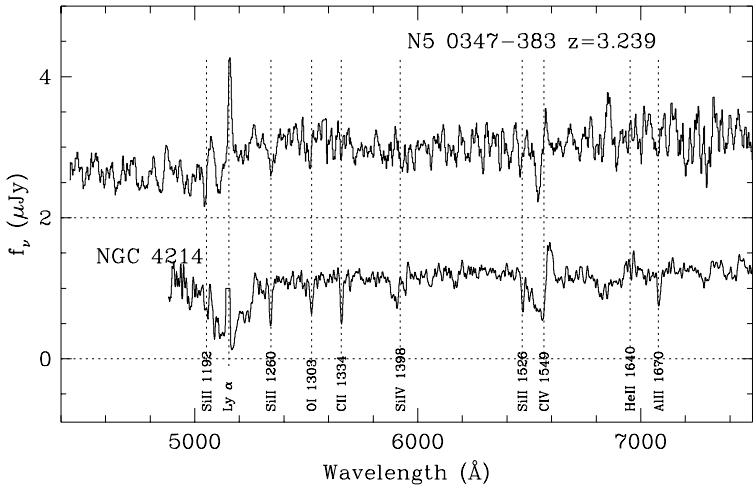

Figure 2: UV spectrum of a $z > 3$ galaxy (upper part). For comparison, a recent HST spectrum of the central starburst region in the Wolf-Rayet galaxy NGC 4214 is also shown (lower part). Note the characteristic P-Cygni lines, especially of C IV and Si IV, pointing to the dominating influence of massive O stars. Figure from Steidel et al. 1996.

The characteristic P-Cygni lines observed as broad stellar wind lines, especially those of the resonance lines of C IV and Si IV, integrated over the stellar populations in the spectra of starbursting galaxies, allow quantitative spectroscopic studies of the most luminous stellar objects in distant galaxies even at high redshift. Thus, in principle, we are able to obtain important quantitative information about the host galaxies of these objects, but diagnostic issues of these spectra require among other things *synthetic UV spectra of O-type stars* as input for the population synthesis calculations needed for a comparison with the observed integrated spectra.

The potential of these spectra for astrophysical diagnostics can nevertheless be investigated in a first step by using *observed* UV spectra of nearby O-type stars as input for the corresponding population synthesis calculations instead. In the frame of this method stars are simulated to form according to a specified star-formation history and initial mass function and then follow predefined tracks in the HR-diagram. The integrated spectra are then built up from a library of observed UV spectra of hot stars in the Galaxy and the Magellanic Clouds. The output of this procedure are semi-empirical UV spectra between 1000 and 1800 Å at 0.1 to 0.7 Å resolution for populations of arbitrary age, star-formation histories, and initial mass function. The computational technique of this method is described comprehensively in the literature and we refer the reader to one of the latest papers of a series (Leitherer et al. 2001).

As an example of the analyses performed in this way a comparison of the average spectrum of 8 clusters in NGC 5253 to synthetic models at solar (top) and 1/4 solar (bottom) metallicity is shown in Figure 3 (Leitherer et al. 2001). The Figure shows clearly that a representative value of the overall metallicity of this starburst galaxy can be determined, since the model spectrum in the lower part fits the observation

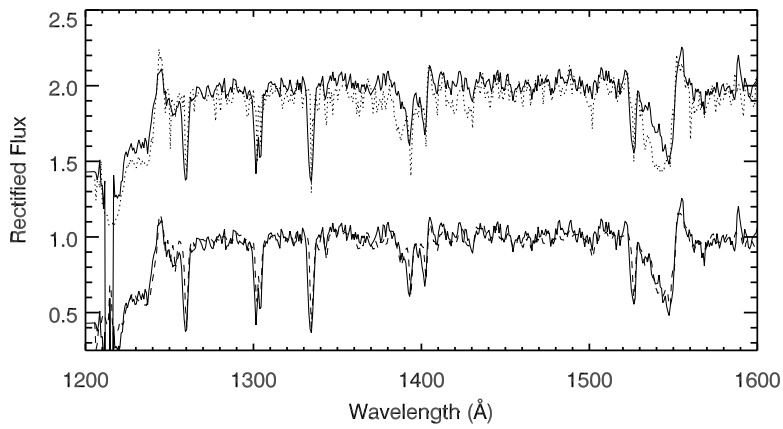

Figure 3: Average spectrum of 8 clusters in NGC 5253 compared to that of a population model at solar (top) and 1/4 solar metallicity (bottom). It is clearly shown that a representative value of the overall metallicity of this starburst galaxy can be determined. Figure from Leitherer et al., 2001.

almost perfectly. This result is especially convincing as both models (dashed lines) are based on the same parameters, except for the metallicity. A standard Salpeter IMF between 1 and 100 $M_\odot$ was used and the starburst has been assumed to last 6 Myr, with stars forming continuously during this time. The worse fit to the observations produced by the solar metallicity model spectrum – particularly discrepant are the blue absorption wings in Si IV and C IV which are too strong in the models – could be improved by reducing the number of the most massive stars with a steeper IMF, but at the cost of the fit quality in the emission components. As an important result the ratio of the absorption to the emission strengths is therefore a sensitive indicator for the metallicity.

Moreover, the strong sensitivity of the emission parts of the P-Cygni lines of N V, Si IV, and C IV on the evolutionary stage of the O stars makes these spectra quite suitable as age tracers, which is shown in Figure 4, where the time evolution of the integrated spectrum following an instantaneous starburst is presented. The line profiles gradually strengthen from a main-sequence-dominated population at 0–1 Myr to a population with luminous O supergiants at 3–5 Myr; and the lines weaken again at later age due to termination of the supergiant phase – this behavior is especially visible in the shape of the C IV $\lambda 1550$ resonance line.

The conclusion from these examples is that this kind of analysis is very promising, but relies on observed UV spectra, which are just available for a small number of metallicity values, namely those of the Galaxy and the Magellanic Clouds. In order to make progress in the direction outlined before, *realistic synthetic UV Spectra of O-type stars* are needed. This is in particular the case for high-redshift galaxies (which are observable spectroscopically when the flux is amplified by gravitational lensing through foreground galaxy clusters) since in these cases the expected metallicities of starbursting galaxies in the early universe (cf. Pettini et al. 2000) are most probably different from local ones.

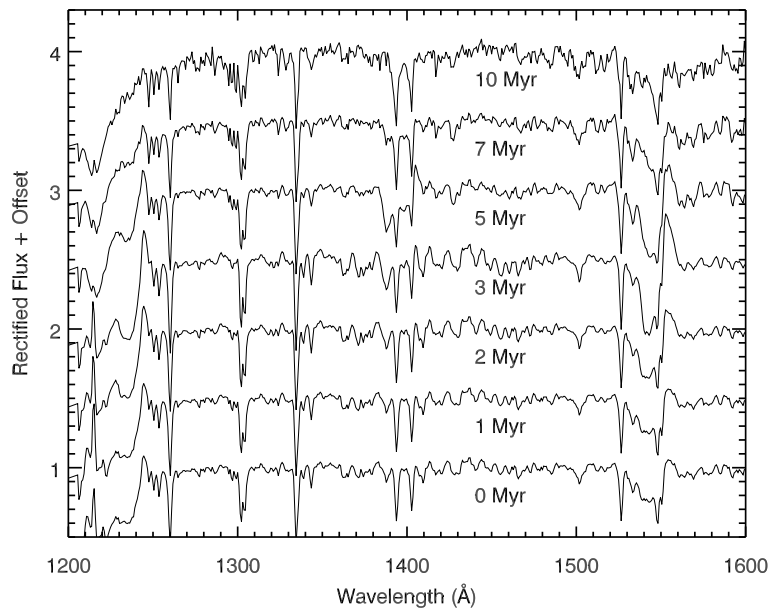

Figure 4: Time evolution of the integrated spectrum for the 10 Myr following an instantaneous starburst. The strong sensitivity of the emission parts of the P-Cygni lines of N V, Si IV, and C IV on the evolutionary stage of the O stars makes these spectra quite suitable as age tracers. Figure from Leitherer et al. 2001.

3 First generations of Stars – Ionization Efficiency of a Top-Heavy Initial Mass Function

Apart from the short evolutionary timescale of massive stars it is obviously the metallicity, and, connected to this, the steepness of the Initial Mass Function, which is responsible for the rarity of these objects in the present phase of the universe. It has to be the metallicity, because very recently strong evidence has been found that the primordial IMF has favored massive stars with masses $> 10^2 M_\odot$ (cf. Bromm et al. 1999). Thus, in the early universe, when only primordial elements were left over from the Big Bang, nature obviously preferred to form massive stars. This prediction is based on the missing metallicity which leads to a characteristic scale for the density and temperature of the primordial gas, which in turn leads to a characteristic Jeans mass of $M_{\rm J} \sim 10^3 M_\odot$ (Larson 1998).

Finally, due to these physical conditions the Initial Mass Function becomes top-heavy and therefore deviates significantly from the standard Salpeter power-law (see, for instance, Bromm et al. 1999, 2001). Such an early population of very massive stars at very low metallicities (i. e., Population III stars) which have already been theoretically investigated by El Eid et al. (1983), recently turned out to be also relevant to cosmological issues, the most important being the cosmological question of when

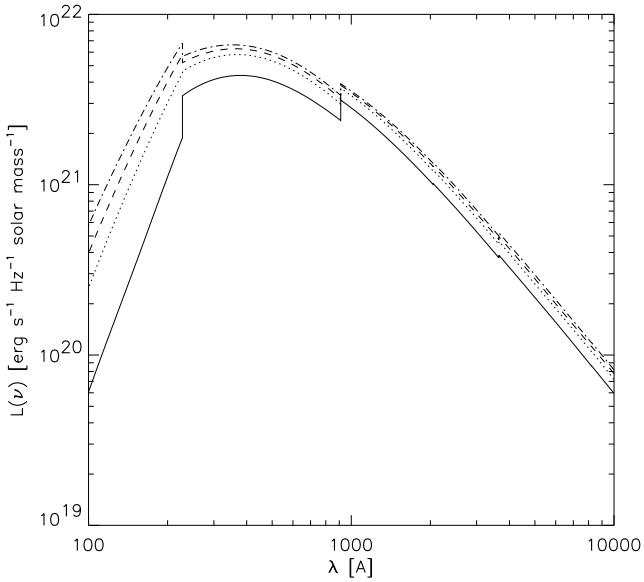

Figure 5: The normalized spectral energy distribution in the continuum of Population III stars – mass range 100–1000 $M_\odot$ at $Z = 0$. Note that the spectra attain an universal form for stellar masses $M > 300\ M_\odot$ Figure from Bromm et al. 2001.

and how the cosmic "dark ages" ended (Loeb 1998). We know that the dark ages ended because the absence of a Gunn-Peterson trough (Gunn and Peterson 1965) in the spectra of high-redshift quasars implies that the universe was reionized again at a redshift of $z > 5.8$ (Fan et al. 2000). For a long time, Carr et al. (1984) suspected that the first generations of stars have been relevant to control this process. Thus, Population III stars could contribute significantly to the ionization history of the intergalactic medium (IGM), but the contribution of the first generation of stars to the ionization history of the IGM depends crucially on their initial mass function. With regard to the first generations of stars the ionization efficiency of a top-heavy Initial Mass Function will, therefore, have to be investigated.

It is the enormous amount of UV and EUV radiation of these very massive stars which could easily change the status of the cold and dark universe at that time to become reionized again. This is indicated in Figure 5, which also shows that the total spectral luminosity depends solely on the total amount of mass, if the mass of the most massive stars exceeds 300 $M_\odot$ (cf. Bromm et al. 2001). Due to this top-heavy Initial Mass Function the total spectral energy distribution deviates significantly from that obtained with the standard Salpeter power-law, as is shown in Figure 6, and the flux obtained can contribute the decisive part to the unexplained deficit of ionizing photons required for the reionization of the universe (cf. Bromm et al. 2001).

However, in order to be able to make quantitative predictions about the influence of this extremely metal poor population of very massive stars on their galactic and intergalactic environment one primarily needs observations that can be compared to the predicted flux spectrum.

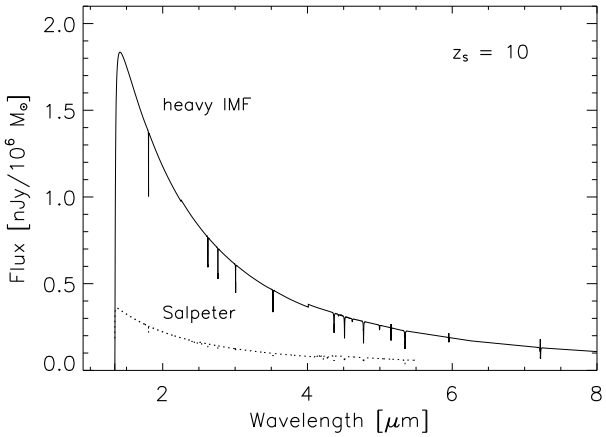

Figure 6: Predicted flux from a Population III star cluster at $z = 10$. A flat universe with $\Omega_\Lambda = 0.7$ is assumed. The cutoff below $\lambda_{\rm obs} = 1216$ Å is due to complete Gunn-Peterson absorption, and the observable flux is larger by an order of magnitude for the case of the top-heavy IMF when compared to the case of the standard Salpeter power-law. Figure from Bromm et al. 2001.

Future observations with the Next Generation Space Telescope of distant stellar populations at high redshifts will principally give us the opportunity to deduce the primordial IMF from these comparisons. Kudritzki (2002) has recently shown that this is generally possible, by calculating state-of-the-art UV spectra for massive O stars in a metallicity range of $1 \ldots 10^{-4}\ Z_\odot$. From an inspection of his spectra he concluded that significant line features are still detectable even at very low metallicities; thus, there will be diagnostic information available to deduce physical properties from starbursting regions at high redshifts that will eventually be observed with the Next Generation Space Telescope in the infrared spectral region.

As a second requirement we need to determine the physical properties of Population III stars during their evolution. A key issue in this regard is to obtain *realistic spectral energy distributions* calculated for metallicities different from zero for the most massive objects, since the assumption of a metallicity of $Z = 0$ is certainly only correct for the very first generation of Population III stars.

4 Theoretical Ionizing Fluxes of O Stars

Although less spectacular, we will now investigate the impact of massive stars on their environment in a more direct manner. Apart from the chemical enrichment of the ISM, the large amount of momentum and energy input into the ambient interstellar medium of these objects is primarily of importance. Especially the radiative energy input shortward of the Lyman edge, which ionizes and heats the Gaseous Nebulae surrounding massive Hot Stars, offers the possibility to analyze the influence of the EUV radiation of the photoionizing stars on the ionization structure of these excited H II regions.

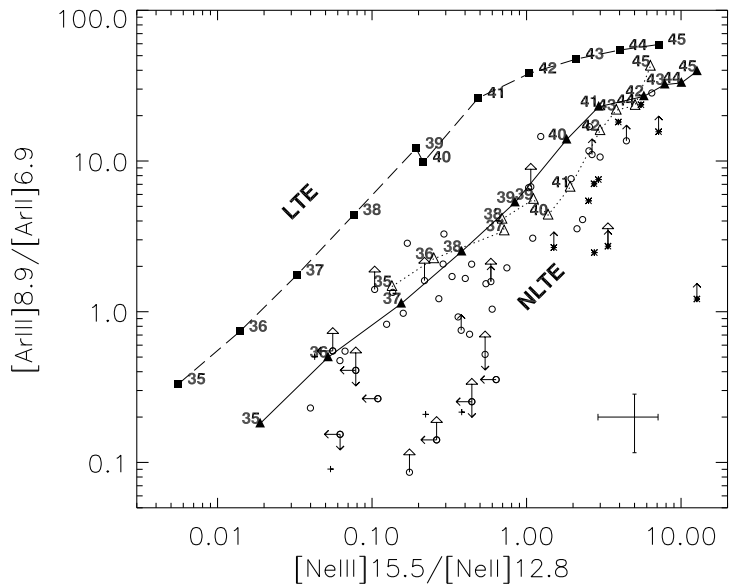

Figure 7: [Ar III] 8.99 μm / [Ar II] 6.99 μm versus [Ne III] 15.6 μm / [Ne II] 12.8 μm diagnostic diagram of observed and predicted nebular excitation of H II regions. Boldface numbers indicate models which are designated by their effective temperature in 10^3 K. Triangles are NLTE models and squares are LTE models; note that the NLTE models represent an impressive improvement in reproducing the [Ne III] emission. A representative error bar for the data is shown in the lower right corner. Figure from Giveon et al. 2002.

The primary objective of such investigations are studies of theoretical models of starburst regions, which for instance are used to determine the energy source in ultra-luminous infrared galaxies – ULIRGs – (cf. Lutz et al. 1996; Genzel et al. 1998). The interpretation of the corresponding extra-galactic observations obviously requires understanding the properties of the spectral energy distributions (SEDs) of massive stars and stellar clusters. Thus, the quality of the SEDs has to be probed in a first step by means of investigations of Galactic H II regions.

4.1 The Excitation of Galactic H II Regions

Giveon et al. (2002) recently presented a comparison of observed [Ne III] 15.6 μm / [Ne II] 12.8 μm and [Ar III] 8.99 μm / [Ar II] 6.99 μm excitation ratios, obtained for a sample of 112 Galactic H II regions and 37 nearby extragalactic H II regions in the LMC, SMC, and M33 observed with ISO-SWS, with the corresponding results of theoretical nebular models.

The authors have chosen infrared fine-structure emission lines for their investigation because these lines do not suffer much from dust extinction and the low energies of the associated levels make these lines quite insensitive to the nebular electron temperature. Moreover, the relative strengths of the fine-structure emission lines chosen are ideal for constraining the shape of the theoretical ionizing fluxes,

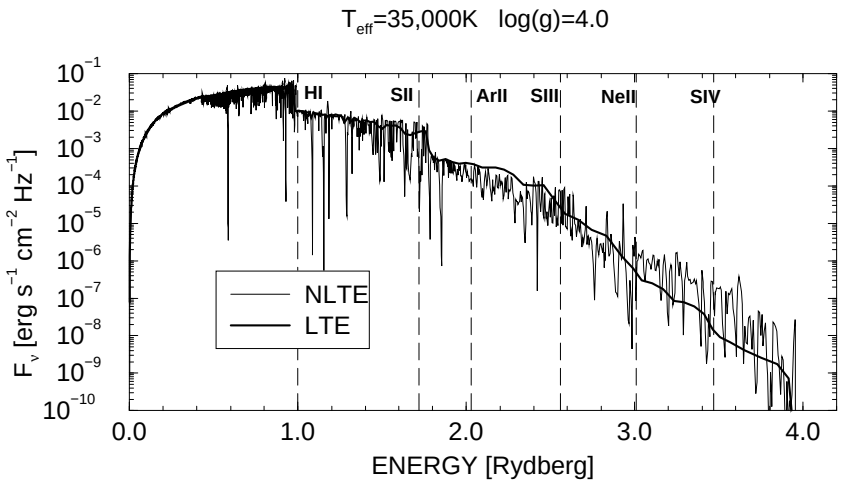

Figure 8: Comparison between the LTE (static atmosphere from Kurucz 1992) and NLTE (expanding atmosphere from Pauldrach et al. 2001) spectral energy distributions of a dwarf with an effective temperature of 35 000 K. The ionization edges of the relevant ions are indicated by vertical dashed lines. It is apparent that the difference in excitation produced by the LTE and NLTE atmospheres will be more pronounced in the Ne^{++}/Ne^{+} ratio than in the Ar^{++}/Ar^{+} ratio. Figure from Giveon et al. 2002.

since the [Ne III] 15.6 μm / [Ne II] 12.8 μm line ratio depends on photons emitted at $\geq$ 3 Rydbergs, while [Ar III] 8.99 μm / [Ar II] 6.99 μm is sensitive to the region $\geq$ 2 Rydbergs. Thus, these line ratios are extremely useful probes of the physical properties of H II regions and their associated ionizing sources especially with regard to the ionizing spectral energy distributions.

The complete set of observed emission line ratios of Ne and Ar is shown in Figure 7 together with the corresponding results of nebular model computations for which solar metallicity and a gas density of 800 cm^{-3} has been assumed, and which are based on LTE (static atmosphere from Kurucz, 1992) as well as NLTE (expanding atmosphere from Pauldrach et al., 2001) spectral energy distributions.

The diagnostic diagram clearly shows that the predicted nebular excitation increases with increasing effective temperature of the photoionizing star, and it also shows that the high excitation [Ne III] emission observed in H II regions is by far not reproduced by nebular calculations which make use of the ionizing fluxes of LTE models – the line ratios are under-predicted by factors larger than 10. This result is clearly an example of the well-known Ne III problem (cf. Baldwin et al. 1991; Rubin et al. 1991; Simpson et al. 1995).

It is quite evident, however, that the quality of the diagnostics depends primarily on the quality of the input, i. e., the spectral energy distributions. It is therefore a significant step forward that the ionizing fluxes of the NLTE models used represent an impressive improvement to the observed excitation correlation – note that the fit shown in Figure 7 may actually be even better, since a lot of the scatter is due to underestimated extinction corrections for the [Ar III] 8.99 μm line. The NLTE sequence

also indicates that for most of the considered H II regions the effective temperatures of the exciting stars lie in the range of 35 000 to 45 000 K. Most importantly, the NLTE models can readily account for the presence of high excitation [Ne III] emission lines in nebular spectra. This result resolves the long-standing Ne III problem and supports the conclusion of Sellmaier et al. (1996), who found, for the first time, on the basis of a less comprehensive sample of H II regions and models that this problem has been the failure of LTE photoionization simulations primarily due to a significant under-prediction of Lyman photons above 40 eV. This issue is solved by making use of NLTE model atmospheres.

The reason for this improvement are the spectral shapes of the NLTE fluxes shortward of the Ar II and Ne II ionization thresholds which are obviously somewhat more realistic in the NLTE case. This is illustrated in Figure 8 where the spectral energy distributions of an LTE and an NLTE model are compared by example of a dwarf with an effective temperature of 35 000 K. As is shown, the SEDs harden in the NLTE case, meaning that the LTE model produces much less flux above the Ne^+ 40.96 eV threshold than the NLTE model. This is the behavior that is essentially represented in the excitation diagram.

4.2 Spectral Energy Distributions of Time-Evolving Stellar Clusters

The improvement obtained for the diagnostic diagram of the analysis of Galactic H II regions in Section 4.1 also has important implications for determining extragalactic abundances and population histories of starburst galaxies.

With regard to this, Thornley et al. (2000) carried out detailed starburst modelling of the [Ne III] 15.6 μm / [Ne II] 12.8 μm ratio of H II regions ionized by clusters of stars. As was shown above, the hottest stars in such models are responsible for producing large nebular [Ne III] 15.6 μm / [Ne II] 12.8 μm ratios. Hence, the low ratios actually observed led to the conclusion that the relative number of hot stars is small due to aging of the starburst systems. Thus, the solution of the Ne III problem has important consequences for the interpretation of these extragalactic fine-structure line observations, since the conclusion that due to the low [Ne III] 15.6 μm / [Ne II] 12.8 μm ratios obtained, the hottest stars as dominant contributors to the ionization of the starburst galaxies have to be removed, has obviously to be proven.

In order to tackle this challenge, Sternberg et al. (2002) computed spectral energy distributions of time-evolving stellar clusters, on the basis of a large grid of calculated NLTE spectral energy distributions of O and early B-type stars (being the major contributors to the Lyman and He I fluxes) in the hot, luminous part ($T_{\rm eff} >$ 25 000 K) of the HR diagram. From this grid, models of stars following evolutionary tracks are suitably interpolated. The SEDs used rely on recent improvements of modelling expanding NLTE atmospheres of Hot Stars (Pauldrach et al. 2001). As an example of the individual models used, Figure 9 shows the calculated spectral energy distribution of a typical O star compared to the corresponding result of an NLTE model of Schaerer and de Koter (1997).

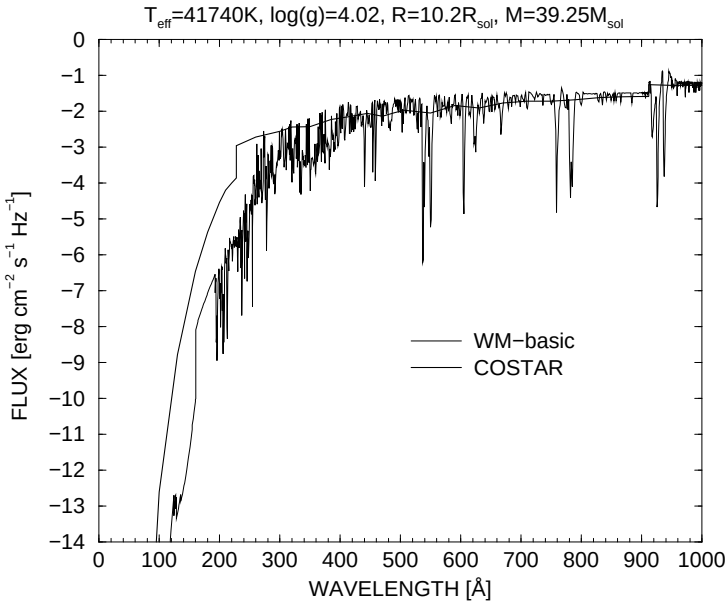

Figure 9: Calculated spectral energy distribution of a typical O star. The spectrum represents the result of the WM-basic model (Pauldrach et al. 2001), and the thick line represents the result of a corresponding COSTAR model (Schaerer and de Koter 1997).

The spectral energy distributions have been calculated for two modes of cluster evolution, a *continuous* and an *impulsive* one. The different spectral evolutions of these modes are shown in Figure 10 with regard to the spectral range of 0.8–2.5 Rydbergs.

In the continuous mode, the star-formation rate is assumed to be constant with time – on time scales which are longer than the lifetimes of massive stars – and the cluster is assumed to form stars at a rate of 1 $M_\odot$ per year. In the impulsive mode, all stars are formed "instantaneously", i. e., on time scales which are much shorter than the lifetimes of massive stars; the total mass of stars formed is $10^5\ M_\odot$, and the cluster is assumed to evolve passively thereafter. Furthermore, the computations are based on a Salpeter initial mass function, where for each mode two cases are assumed, one with an upper mass limit of $M_{\rm up} = 120\ M_\odot$ and the other one with an upper mass limit of $M_{\rm up} = 30\ M_\odot$.

Two striking effects are seen in Figure 10:

1. In the continuous mode, the cluster ionizing spectrum becomes softer – i.e., steeper – between 1 and 10 Myr. This is due to the increase of the relative number of late versus early-type OB stars during the evolution, since the less massive late-type stars have longer lifetimes. This effect is particularly noticeable for the cluster model with $M_{\rm up} = 120\ M_\odot$.

2. In the impulsive mode, the magnitude of the Lyman break increases drastically because the massive stars disappear with time.

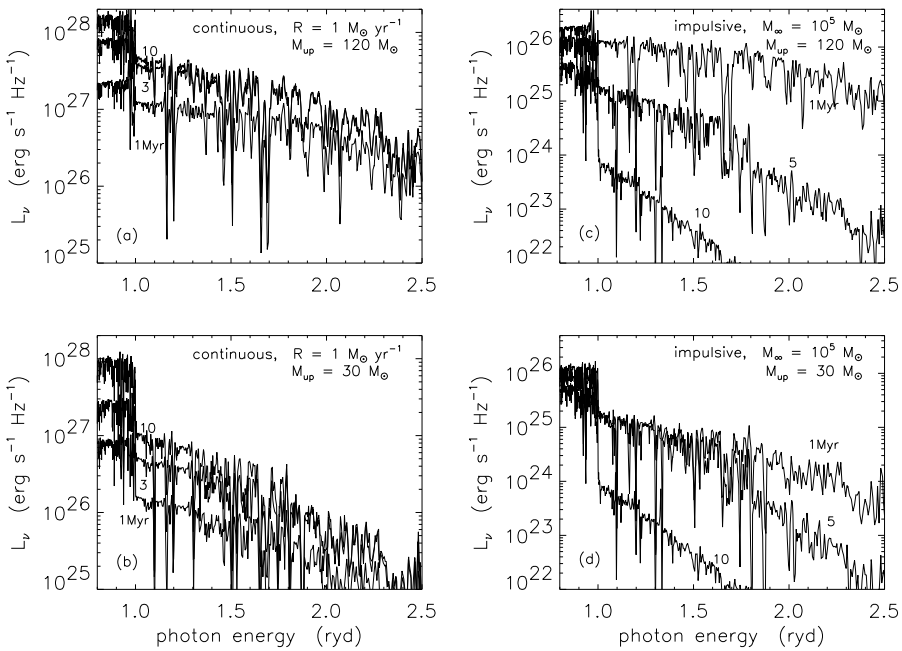

Figure 10: Spectral energy distributions of time-evolving stellar clusters. Two modes of cluster evolution are shown: *continuous* and *impulsive*. *(Left)*: Evolution for continuous star formation (lasting 10^{10} yr) for two extreme stellar compositions. In the upper panel evolving SEDs of a cluster with $M_{\rm up} = 120\ M_\odot$, and in the lower panel with $M_{\rm up} = 30\ M_\odot$ are shown. Note that at early phases the amount of both ionizing and non-ionizing photons increase due to the increasing number of new-formed stars. After a time period of ~ 5 Myr the number of ionizing photons remains roughly constant, because an equilibrium of stellar aging and stellar birth is achieved, whereas the number of non-ionizing photons remains proportional to age, because of accumulation effects of old stars which are the major contributors to this spectral range. *(Right)*: Evolution of an impulsive star formation burst (lasting 10^5 yr), for the same extreme stellar compositions as above. Note that the ionizing photons practically disappear at an age of ~ 10 Myr. Figure from Sternberg et al. 2002.

The evolution of the photon emission rates for photons above the Lyman ($Q_{\rm H}$) and the He I ($Q_{\rm He}$) ionization thresholds is shown in Figure 11 for both modes of the clusters. The key difference between the two modes leads to completely different shapes of the photon emission rates, which will be easy to distinguish in view of their photoionizing properties acting on their gaseous environments. It is also shown that increasing the upper IMF mass cut-off increases the photon emission rates, but does not change the shapes of the rates obtained during the evolution. The methods developed for determining extragalactic abundances and population histories from an analysis of H II regions are thus very promising.

From these investigations it is obvious that realistic spectral energy distributions of massive stars and stellar clusters are important for studies of their environments. The crucial question, however, whether the spectral energy distributions of massive

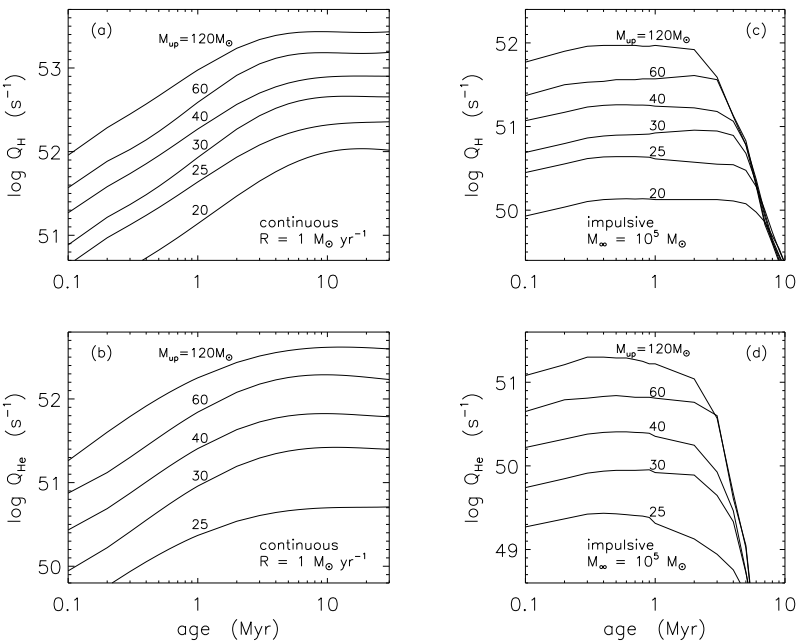

Figure 11: Evolution of the Lyman and He I photon emission rates for a range of values of the upper IMF mass cut-off. The continuous star formation mode is considered on the left hand side, and the impulsive star formation burst on the right. Figure from Sternberg et al. 2002.

stars are already realistic enough to be used for diagnostic issues of H II regions has not been answered yet, since on the basis of the results obtained for the diagnostic diagram in Section 4.1 it cannot be excluded that wrong fluxes could show the same improvements in the Ne^{++}/Ne^{+} ratios just by chance.

An answer to this question requires an *ultimate test*!

This ultimate test is only provided by comparing the observed and synthetic UV spectra of the individual massive stars, based on the following reasons:

1. This test involves hundreds of spectral signatures of various ionization stages with different ionization thresholds which cover a large frequency range.

2. Almost all of the ionization thresholds lie within the spectral range shortward of the Lyman ionization threshold (cf. Figure 12); thus, *the ionization balances of all elements depend sensitively on the ionizing radiation throughout the entire wind*.

The ionization balance can be traced reliably through the strength and structure of the wind lines formed throughout the atmosphere. Hence, it is a natural and the only reliable step to test the quality of the ionizing fluxes by virtue of their direct product: *the UV spectra of O stars*.

But before we turn to this test we will continue our discussion with another astrophysically important stellar object.

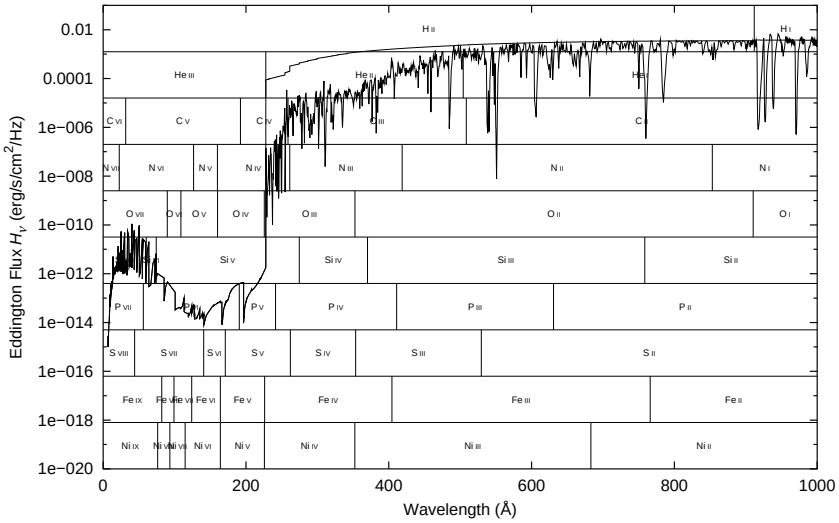

Figure 12: Spectral energy distribution shortward of the Lyman ionization threshold of an expanding NLTE model atmosphere for an O supergiant (Pauldrach et al. 2003). The small vertical bars indicate the ionization thresholds for all important ions; the ionization balance depends almost entirely on the ionizing flux, and this influence can be traced by the spectral lines in the observable part of the UV spectrum.

5 Supernovae of Type Ia as Distance Indicators

In order to complete the discussion of Hot Stars in the context of modern astronomy, we will concentrate now on the subject of Supernovae of Type Ia. With respect to diagnostic issues we will investigate the role of Supernovae of Type Ia as distance indicators. The context of this discussion regards, as a starting point, the current surprising result that distant SNe Ia at intermediate redshift appear fainter than standard candles in an empty Friedmann model of the universe.

Type Ia supernovae, which are the result of the thermonuclear explosion of a compact low mass star, are currently the best known distance indicators. Due to their large luminosities ($L_{\max} \sim 10^{43}$ erg/s) they reach far beyond the local supercluster (cf. Saha et al. 2001 and references therein). It is thus not surprising that Type Ia supernovae have become the most important cosmological distance indicator over the last years, and this is not only due to their extreme brightness, but primarily due to their maximum luminosity which can be normalized by their light curve shape, so that these objects can be regarded as *standard candles*. This has been shown by observations of local SNe Ia which define the linear expansion of the local universe extremely well (Riess et al. 1999), which in turn is convincing proof of the accuracy of the measured distances. On the other hand, observations of distant SNe Ia (up to redshifts of about 1) have yielded strong evidence that the expansion rate has been accelerated 6 Gyr ago (cf. Riess et al. 1998 and Perlmutter et al. 1999).

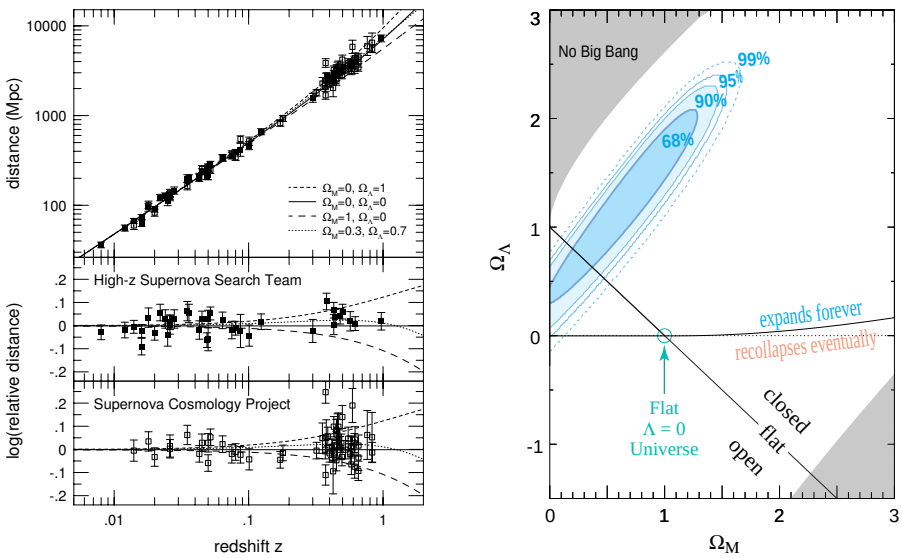

Figure 13: *Left*: Hubble diagram of Type Ia Supernovae. In the upper panel the distance modulus versus redshift is shown in the usual way, whereas the distance modulus has been normalized to an empty universe in the lower panels. Shown are the data of the High-z SN Search Team (filled squares; Riess et al. 1998) and the Supernova Cosmology Project (open squares; Perlmutter et al. 1999). In addition, lines of four cosmological models are drawn, where the full line corresponds to a cosmological model for an empty universe and the dotted line to a flat universe. Figure from Leibundgut 2001.
Right: Cosmological diagram showing the likelihood region as defined by SNe Ia in the Ω_Λ versus $\Omega_{\rm Mass}$ plane. The results of 79 SNe Ia have been included – 27 local and 52 distant ones – from the sources above. Contours indicate 68 %, 90 %, 95 %, and 99 % probability, and the line for a flat universe is indicated. Note that the SN Ia luminosity distances clearly indicate an accelerated expansion of the universe. Figure from Perlmutter et al. 1999.

This surprising result becomes evident if we look at the Hubble diagram in the form of distance modulus versus redshift (cf. Figure 13). As is shown in the diagrams of the lower panels, which are normalized to a cosmological model for an empty universe, most SNe Ia at intermediate redshift are positioned at positive values of the normalized distance modulus; thus, the distant supernovae appear fainter than what would be expected in a empty universe. This means that deceleration from gravitational action of the matter content does not take place. Moreover, the SNe Ia appear even more distant indicating an accelerated expansion over the last 6 Gyr.

The implications of this are immediately recognized in the cosmological diagram on the right-hand side of Figure 13, where Ω_Λ versus $\Omega_{\rm Mass}$ is plotted. The SN Ia results obviously exclude any world model with matter but without a a cosmological constant. Hence, the data show the need for an energy contribution by the vacuum. Thus, the SN luminosity distances indicate accelerated expansion of the universe!

However, this is not the only interpretation of the result obtained. There are other astrophysical explanations, such as obscuration by intergalactic dust or evolution of

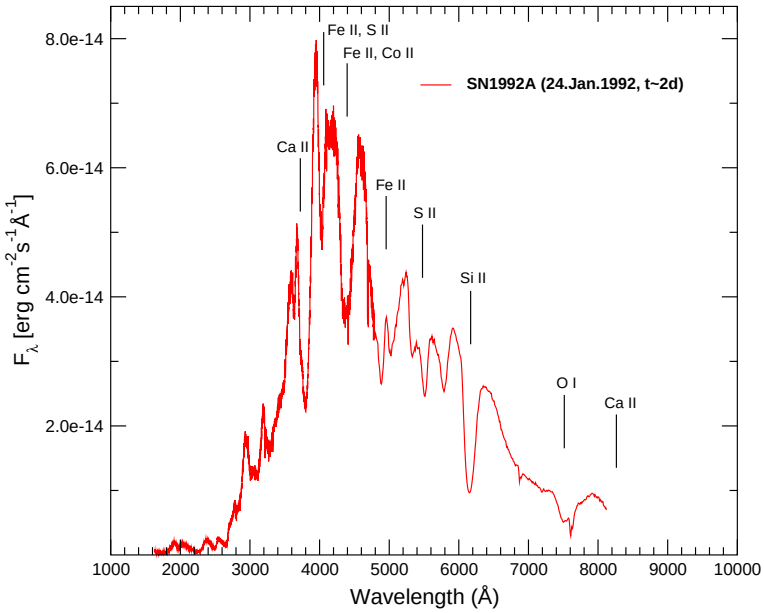

Figure 14: Observed HST spectrum of a standard Supernova of Type Ia at early phase – SN 1992A from 24 Jan. 1992. Figure from Kirshner et al. 1993.

supernovae of Type Ia (cf. Leibundgut 2001). The latter point refers primarily to the absolute peak luminosity of SNe Ia which might have changed between the local epoch and a redshift of 1.0, especially in the case of a decrease: then the fainter supernovae would not be a signature of larger distances, but rather of an evolution of these objects. Although present SN Ia models do not favor such an evolution, it cannot be excluded, because neither the explosions nor the radiation emerging from the atmosphere are understood in detail yet. Consequently, serious caveats for the cosmological interpretation of distant supernovae exist.

Thus, we are faced with the question: Are SNe Ia standard candles independent of age, or is there some evolution of the SN luminosity with age? Among other things spectroscopy is certainly a powerful tool to obtain an answer to this question by searching for spectral differences between local and distant SNe Ia.

Unfortunately, at present, we do not have a clear picture of the exact physical processes which take place in a SN Ia explosion and how the radiation released from it should be treated (for a recent review see Hillebrandt and Niemeyer 2000). In order to get an impression of the basic physics involved that affect the atmospheric structure of a SN Ia, a quick glance at an observed spectrum will help to point out the necessary steps for their further analysis.

Figure 14 shows a typical SN Ia spectrum at early epochs ($<$ 2 weeks after maximum). The most striking features of this spectrum are the characteristic P Cygni line profiles which are quite similar to the signatures of O stars. But compared to the latter objects there are also important differences: the broad lines indicate that the velocities of the SN Ia ejecta are almost a factor of 10 larger (up to 30 000 km/s)

and, as a second important point, SN Ia spectra contain no H and He lines. Instead, prominent absorption features of mainly intermediate-mass elements (Si II, O I, S II, Ca II, Mg II, ...) embedded in a non-thermal pseudo-continuum are observed.

To answer the question of whether SN Ia are standard candles in a cosmological sense, realistic models and synthetic spectra of Type Ia Supernovae are obviously required for the analysis of the observed spectra. As just shown, however, these models will necessarily need to be based on a similar serious approach for expanding atmospheres, characterized by non-equilibrium thermodynamics, as is the case for Hot Stars in general.

It will be shown in Section 7.1 that such spectra are in principle already available.

6 Concept for Consistent Models of Hot Star Atmospheres

In order to determine stellar abundances, parameters, and physical properties (and from these, obtain realistic spectral energy distributions) of Hot Stars via quantitative UV spectroscopy, a principal difficulty needs to be overcome: *the diagnostic tools and techniques must be provided*. This requires the construction of detailed atmospheric models.

As has been demonstrated in the previous sections, such a tool has not been made obsolete by general development in astrophysics. On the contrary, it is becoming more and more relevant to current astronomical research as spectral analysis of hot luminous stars is of growing astrophysical interest. Thus, continuing effort is expended to develop a standard code in order to provide the necessary diagnostic tool. In the following part of this section we describe the status of our continuing work to construct realistic models for expanding atmospheres.

Before we focus on the theory in its present stage, we should mention previous fundamental work which turned out to be essential in elaborating the theory. In this context I want to emphasize publications which refer to key aspects of theoretical activity. The starting point of the development of the radiation-driven wind theory is rooted in a paper by Milne (1926) more than 70 years ago. Milne was the first to realize that radiation could be coupled to ions and that this process subsequently may eject the ions from the stellar surface. The next fundamental step goes back to Sobolev (1957), who developed the basic ideas of radiative transfer in expanding atmospheres.

Radiation pressure as a driving mechanism for stellar outflow was rediscovered by Lucy and Solomon (1970) who developed the basis of the theory and the first attempt to its solution. The pioneering step in the formulation of the theory in a quasi self-consistent manner was performed by Castor, Abbott, and Klein (1975). Although these approaches were only qualitative (due to many simplifications), the theory was developed further owing to the promising results obtained by these authors. Regarding key aspects of the solution of the radiative transfer the work of Rybicki (1971) and Hummer and Rybicki (1985) has to be emphasized. With respect to the soft X-ray emission of O stars (detected by Seward et al. 1979 and Harnden et al. 1979), Cassinelli and Olson (1979) have investigated the possible influence of X-rays

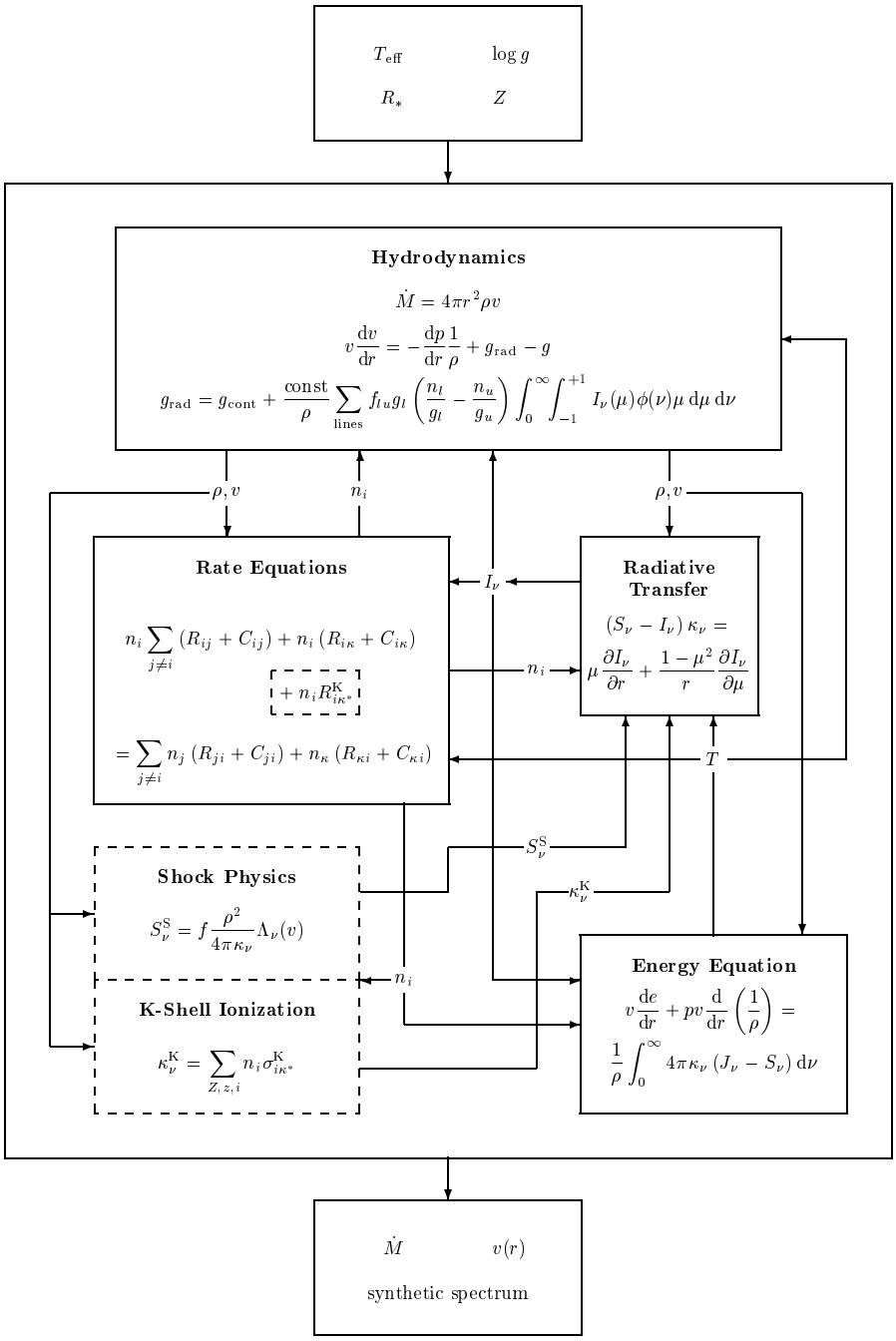

Figure 15: Schematic sketch of the basic equations and the non-linear system of integro-differential equations that form the basis of stationary models of hot star atmospheres – for details see text. Figure from Pauldrach et al. 1994b).

on the ionization structure. Finally, Lucy and White (1980) and Owocki, Castor, and Rybicki (1988) have distinguished themselves with basic theoretical investigations of time-dependent radiation hydrodynamics which describe the creation and development of shocks (for more details about the role of X-rays in the atmospheres of Hot Stars see the reviews of Pauldrach et al. 1994b and Kudritzki and Puls 2000).

6.1 The general method

The basis of our approach in constructing detailed atmospheric models for Hot Stars is the concept of *homogeneous, stationary, and spherically symmetric radiation driven winds*, where the expansion of the atmosphere is due to scattering and absorption of Doppler-shifted metal lines. Although these approximations seem to be quite restrictive, it has already been shown that the time-averaged mean of the observed UV spectral features can be described correctly by such a method (Pauldrach et al. 1994, 1994b).

The primary output of this kind of model calculation are the spectral energy distributions and synthetic spectra emitted by the atmospheres of hot stars. As these spectra consist of hundreds of strong and also weak wind-contaminated spectral lines which form the basis of a quantitative analysis, and as the spectral energy distribution from hot stars is also used as input for the analysis of emission line spectra which depend sensitively on the structure of the emergent stellar flux (cf. Section 4), a sophisticated and well-tested method is required to produce these data sets accurately.

However, developing such a method is not straightforward, since modelling the atmospheres of hot star involves the replication of a tightly interwoven mesh of physical processes: the equations of radiation hydrodynamics including the energy equation, the statistical equilibrium for all important ions with detailed atomic physics, and the radiative transfer equation at all transition frequencies have to be solved simultaneously. Figure 15 gives an overview of the physics to be treated.

The principal features are:

(1) *The stellar parameters* $T_{\rm eff}$ (effective temperature), $\log g$ (logarithm of photospheric gravitational acceleration), R_* (photospheric radius defined at a Rosseland optical depth of 2/3) and Z (abundances) have to be pre-specified.

(2) *The hydrodynamic equations* are solved (r is the radial coordinate, ϱ the mass density, v the velocity, p the gas pressure and $\dot{M}$ the mass loss rate). The crucial term is the radiative acceleration $g_{\rm rad}$ with minor contributions from continuous absorption and major contributions from scattering and line absorption. For each line the oscillator strengths f_{lu}, the statistical weights g_l, g_u, and the occupation numbers n_l, n_u of the lower and upper level enter the equations, together with the frequency and angle integral over the specific intensity I_ν and the line broadening function φ_ν accounting for the Doppler effect.

(3) *The occupation numbers* are determined by the *rate equations* containing collisional (C_{ij}) and radiative (R_{ij}) transition rates. Low-temperature dielectronic recombination is included and Auger ionization due to K-shell absorption (essential for C, N, O, Ne, Mg, Si, and S) of soft X-ray radiation arising from

shock-heated matter is taken into account using detailed atomic models for all important ions. Note that the hydrodynamical equations are coupled directly with the rate equations. The velocity field enters into the radiative rates while the density is important for the collisional rates and the equation of particle conservation. On the other hand, the occupation numbers are crucial for the hydrodynamics since the radiative line acceleration dominates the equation of motion.

(4) *The spherical transfer equation* which yields the radiation field at every depth point, including the thermalized layers where the diffusion approximation is applied, is solved for the total opacities (κ_ν) and source functions (S_ν) of all important ions. Hence, the influence of the spectral lines – the strong EUV *line blocking* – which affects the ionizing flux that determines the ionization and excitation of levels, is taken into account. Note that the radiation field is coupled with the hydrodynamics ($g_{\rm rad}$) and the rate equations (R_{ij}).

Moreover, the *shock source functions* ($S_\nu^{\rm S}$) produced by radiative cooling zones which originate from a simulation of shock heated matter, together with K-shell absorption ($\kappa_\nu^{\rm K}$), are also included in the radiative transfer. The shock source function is incorporated on the basis of an approximate calculation of the volume emission coefficient (Λ_ν) of the X-ray plasma in dependence of the velocity-dependent post-shock temperatures and the filling factor (f).

(5) *The temperature structure* is determined by the microscopic *energy equation* which, in principle, states that the luminosity must be conserved. *Line blanketing* effects which reflect the influence of line blocking on the temperature structure are taken into account.

(6) The iterative solution of the total system of equations yields the hydrodynamic structure of the wind (i. e., the *mass-loss rate* $\dot{M}$ and the *velocity structure* $v(r)$) together with *synthetic spectra* and ionizing fluxes.

Essential steps which form the basis of the theoretical framework developed are described in Pauldrach et al. 1986, Pauldrach 1987, Pauldrach and Herrero 1988, Puls and Pauldrach 1990, Pauldrach et al. 1994, Feldmeier et al. 1997, and Pauldrach et al. 1998.

The effect complicating the system the most is the overlap of the spectral lines. This effect is induced by the velocity field of the expanding atmosphere which shifts at different radii up to 1000 spectral lines of different ions into the line of sight at each observer's frequency. Since the behavior of most of the UV spectral lines additionally depends critically on a detailed and consistent description of the corresponding effects of *line blocking* and *line blanketing* (cf. Pauldrach 1987), special attention has to be given to the correct treatment of the Doppler-shifted line radiation transport of all metal lines in the entire sub- and supersonically expanding atmosphere, the corresponding coupling with the radiative rates in the rate equations, and the energy conservation. Another important point to emphasize concerns the atomic data, since it is quite obvious that the quality of the calculated spectra, the multilevel NLTE treatment of the metal ions (from C to Zn), and the adequate representation

of line blocking and the radiative line acceleration depends crucially on the quality of the atomic models. Thus, the data have to be continuously improved whenever significant progress of atomic data modelling is made. Together with a revised inclusion of EUV and X-ray radiation produced by cooling zones which originate from the simulation of shock heated matter, these improvements have been implemented and described in a recent paper (Pauldrach et al. 2001). Very recently we have additionally focused on a remaining aspect regarding hydrodynamical calculations which are consistent with the radiation field obtained from the line-overlap computations, and we have incorporated this improvement into our procedure (see Pauldrach and Hoffmann 2003).

This solution method is in its present stage already regarded as a standard procedure towards a realistic description of stationary wind models. Thus, together with an easy-to-use interface and an installation wizard, the program package *WM-basic* has been made available to the community. The package can be downloaded from the URL given on the first page.

In the next section we will investigate thoroughly whether these kind of models already lead to realistic results.

7 Synthetic Spectra and Models of Hot Star Atmospheres

The first five sections of this review inevitably lead to the realization that line features of expanding atmospheres are one of the most important astronomical manifestations, since they can easily be identified even in spectra of medium resolution in individual objects like supernovae or in integrated spectra of starburst regions even at significant redshift. As a consequence, they can be used to provide important information about the chemical composition, the extragalactic distance scale, and several other properties of miscellaneous stellar populations. All that is required are *hydrodynamic NLTE model atmospheres* that incorporate the effects of spherical extension and expansion as realistic and consistent as possible. After almost two decades of work these model atmospheres now seem to be available, and in the following we will investigate thoroughly whether basic steps towards realistic synthetic spectra for Supernovae of Type Ia can already be presented, and whether UV diagnostic techniques applied to two of the most luminous O supergiants in the Galaxy lead to synthetic spectra which can be regarded as a measure of excellent quality.

7.1 Synthetic and Observed Spectra of Supernovae of Type Ia

Prominent features in the spectra of Type Ia supernovae in early phases are the characteristic absorption lines resulting from low ionized intermediate-mass elements, such as Si II, O I, Ca II, Mg II, cf. Figure 17. These absorption lines show characteristic line shapes due to Doppler-broadening resulting from the large velocity gradients. The formation of these lines results in a pseudo-continuum that is set up

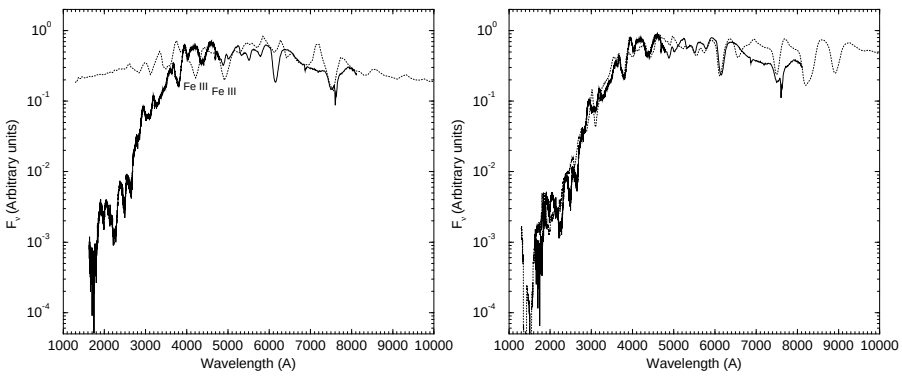

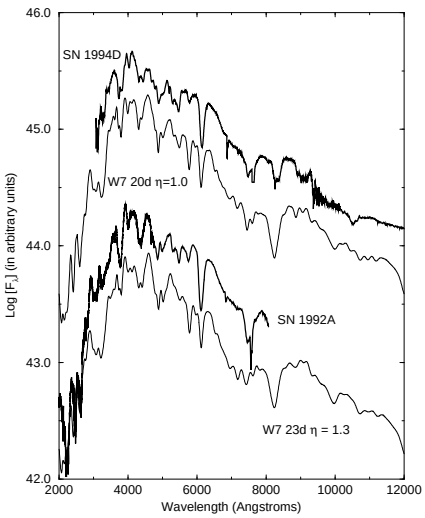

Figure 16: Synthetic NLTE spectra of a Supernova of Type Ia. *Top*: The dotted lines show the spectrum from a model without line blocking (left panel) and from one where line blocking is treated consistently (right panel), both compared to the observed spectrum of SN 1992A (solid line). (Figure from Pauldrach et al. 1996.) *Left*: The two curves in the lower part show a synthetic spectrum for a W7 model at 23 days compared to the observed spectrum of SN 1992A. (Figure from Nugent et al. 1997.) The observed spectrum is from Kirshner et al. 1993 (5 days after maximum light).

by the enormous number of these lines. Supernovae appear in this 'photospheric' epoch for about one month after the explosion and the spectra at this epoch contain useful information on the energetics of the explosion (luminosity, velocity- and density-structure) and on the nucleosynthesis in the intermediate and outer part of the progenitor star. Therefore, the primary objective in order to analyze the spectra is to construct consistent models which link the results of the nucleosynthesis and hydrodynamics obtained from state-of-the-art explosion models (cf. Reinecke et al. 1999) with the calculations of light curves and synthetic spectra of SN Ia. In a first step, however, this is done by using the standard hydrodynamical model W7 by Nomoto et al. 1984. Figure 16 exemplifies the status quo of the synthetic Spectra of Type Ia Supernovae at early phases obtained from this first step, compared to observations.

Obviously, the first comparison shown (top left panel of Figure 16) does not at all represent a realistic atmospheric model. The synthetic spectrum shown has been calculated for a model without line blocking, i. e., only continuum opacity has been considered in the NLTE calculation. Thus, the drastic effects of line blocking on the ionization and excitation and the emergent flux can be verified by comparing the

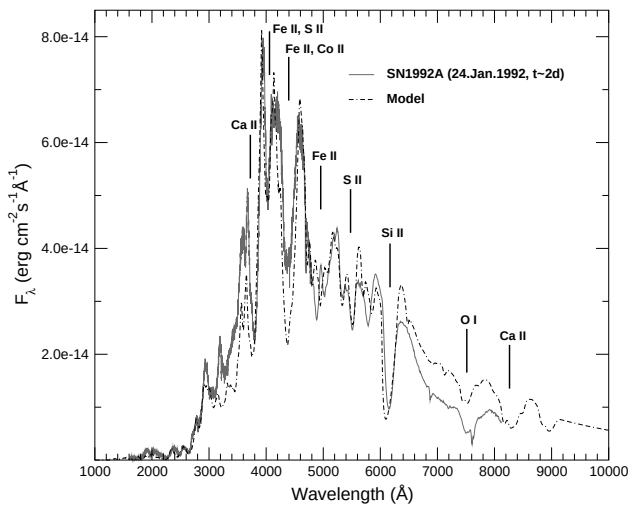

Figure 17: Comparison of the most recent synthetic NLTE spectrum at early phases and the observed spectrum of SN 1992A, illustrating that the method used is already on a quantitative level. The rest wavelengths of various metal lines are indicated by vertical bars. Figure from Sauer and Pauldrach 2002.

calculated flux with the observed flux, where the huge difference in the UV is due to the missing contribution of the lines to the opacity. It is an essential by-product of this result that the observed line features in the optical are also not reproduced: The two strongest features in the synthetic spectrum are due to Fe III lines, indicating that the ionization is too high because of the excessive UV flux. This behavior nicely illustrates that the ionization balance depends almost entirely on the ionizing UV flux and that this influence can be traced by the spectral lines in the observable part of the spectrum, as has been stated in Section 4.2.

The fact that the difference in the UV observed for this model is indeed due to line blocking becomes obvious if this important effect is properly taken into account, as in the case of the model shown in the upper right panel of Figure 16. The agreement of the resulting spectrum of this model with the observations is quite good, demonstrating that line blocking alone can diminish the discrepancy between the synthetic and the observed spectra. Both the flux level and most line features are now reasonably well reproduced throughout the spectrum (cf. Pauldrach et al. 1996). Additionally, in the lower left panel of Figure 16 a spectral fit to the same supernova observation by Nugent et al. (1997) is shown, which is based on a completely independent approach to the theory. The resulting spectrum is also quite reasonable.

Finally, Figure 17 shows a recently calculated synthetic spectrum that is based on the important improvements of the theory described in the previous section, compared to the observed “standard” supernova spectrum (SN 1992A). The synthetic spectrum reproduces the observed spectrum quite well, and the overall impression of this comparison is that the method used is already on a quantitative level, indicating that the basic physics is treated properly (cf. Sauer and Pauldrach 2002).

Although there is still need for improvements regarding, for instance, a proper treatment of the γ energy deposition in the outermost layers and the use of current hydrodynamic explosion models, these models form the basis for the primary objective of the subject, i. e., to search for spectral differences between local and distant SNe Ia. Concerning the facilities of spectral analysis we are thus close to the point where we can tackle the question of whether SNe Ia are standard candles in a cosmological sense.

7.2 Detailed Analyses of Massive O Stars

The objectives of a detailed comparison of synthetic and observed UV spectra of massive O stars are manifold. Primarily it has to be verified that the higher level of consistent description of the theoretical concept of line blocking and blanketing effects and the involved modifications to the models leads to changes in the line spectra with much better agreement to the observed spectra than the previous, less elaborated and less consistent models. Secondly it has to be shown that the stellar parameters, the wind parameters, and the abundances can be determined diagnostically via a comparison of observed and calculated high-resolution spectra covering the observable UV region. And finally, the quality of the spectral energy distributions has to be verified. The latter point, however, is a direct by-product of the other objectives if the complete observed high-resolution UV spectra are accurately reproduced by the synthetic ones, as illustrated in Section 4.2

In the following, the potential of the improved method will be demonstrated by an application to the O4 I(f) star ζ Puppis and the O9.5 Ia star α Cam.

7.2.1 UV Analysis of the Hot O Supergiant ζ Puppis

Referring to the beginning of the review, we will now start to examine carefully the old-fashioned UV spectrum of ζ Puppis. To put this into perspective, we will also briefly review the improvements of UV line fits following from gradual improvements of the methods used.

The first serious attempt to analyze the UV spectrum of this standard object goes back to Lamers and Morton in 1976. From a present point of view their model can not be regarded as a sophisticated one, because they *assumed* the complete model structure – the dynamical structure, the occupation numbers, and the temperature structure – and the line radiative transfer was treated in an approximative way. Nevertheless, we learned from this kind of spectrum synthesis that a solution to the problem is feasible, and that at least the dynamical parameters – the mass-loss rate ($\dot{M}$) and the terminal velocity (v_∞) – can, in principle, be determined from UV lines quite accurately. The UV line fits of Hamann in 1980 have been based on the same assumptions apart from a very detailed treatment of the radiative line transfer. As a result of this the calculated resonance lines of some ions were already quite well in agreement with the observed ones. But the real conclusion to be drawn from these comparisons is that a detailed analysis requires a more consistent treatment of expanding atmospheres.

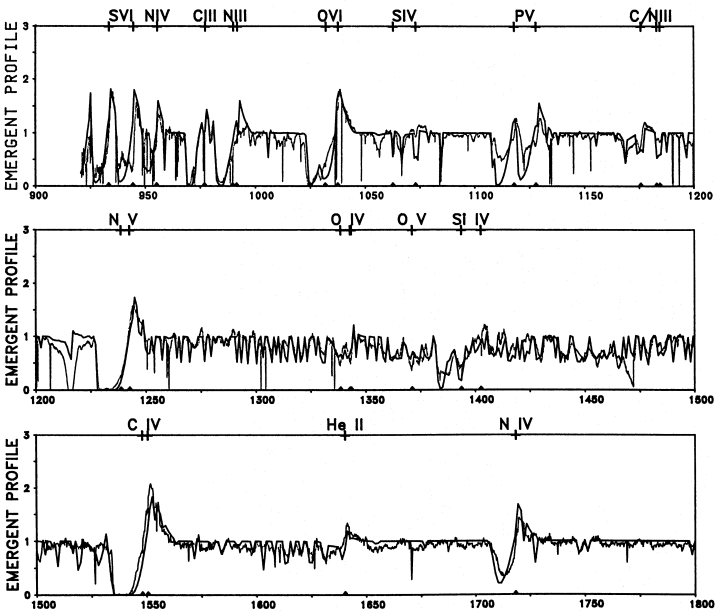

Figure 18: Calculated and observed UV spectrum of ζ Puppis. The observed spectrum shows the Copernicus and IUE high-resolution observations, and the calculated spectrum belongs to the final model of Pauldrach et al. 1994.

The situation improved considerably with the first attempts to find a consistent solution, meaning that the equations of hydrodynamics, non-equilibrium thermodynamics, and radiative transfer have been solved in a consistent way. Pauldrach (1987) introduced for the first time a full NLTE treatment of the metal lines driving the wind, and Puls (1987) investigated the important effect of multiple photon momentum transfer through line overlaps caused by the velocity-induced Doppler-shifts for applications in stellar wind dynamics. From this procedure, dynamical parameters, constraints on the stellar parameters, and, as has been verified by a comparison of a sample of calculated spectral lines with the observed spectrum, an ionization equilibrium and occupation numbers which were close to a correct description have already been obtained. But, among other approximations, the models still suffered from the neglect of radiation emitted from shock cooling zones and from a very approximate treatment of line blocking.

The further steps to reproduce most of the important observed individual line features in the UV required a lot of effort in atomic physics, in improved NLTE multilevel radiative transfer, and in spectrum synthesis techniques. An important step towards this objective was the paper by Pauldrach et al. (1994), where for the first time stellar parameters and abundances have been determined from individual UV line features. Figure 18 shows the corresponding synthetic spectrum that was already in overall agreement with the observations. Nevertheless, the treatment was still affected by a number of severe approximations regarding especially the neglect of the line blanketing effect, an approximate treatment of the line radiative transfer,

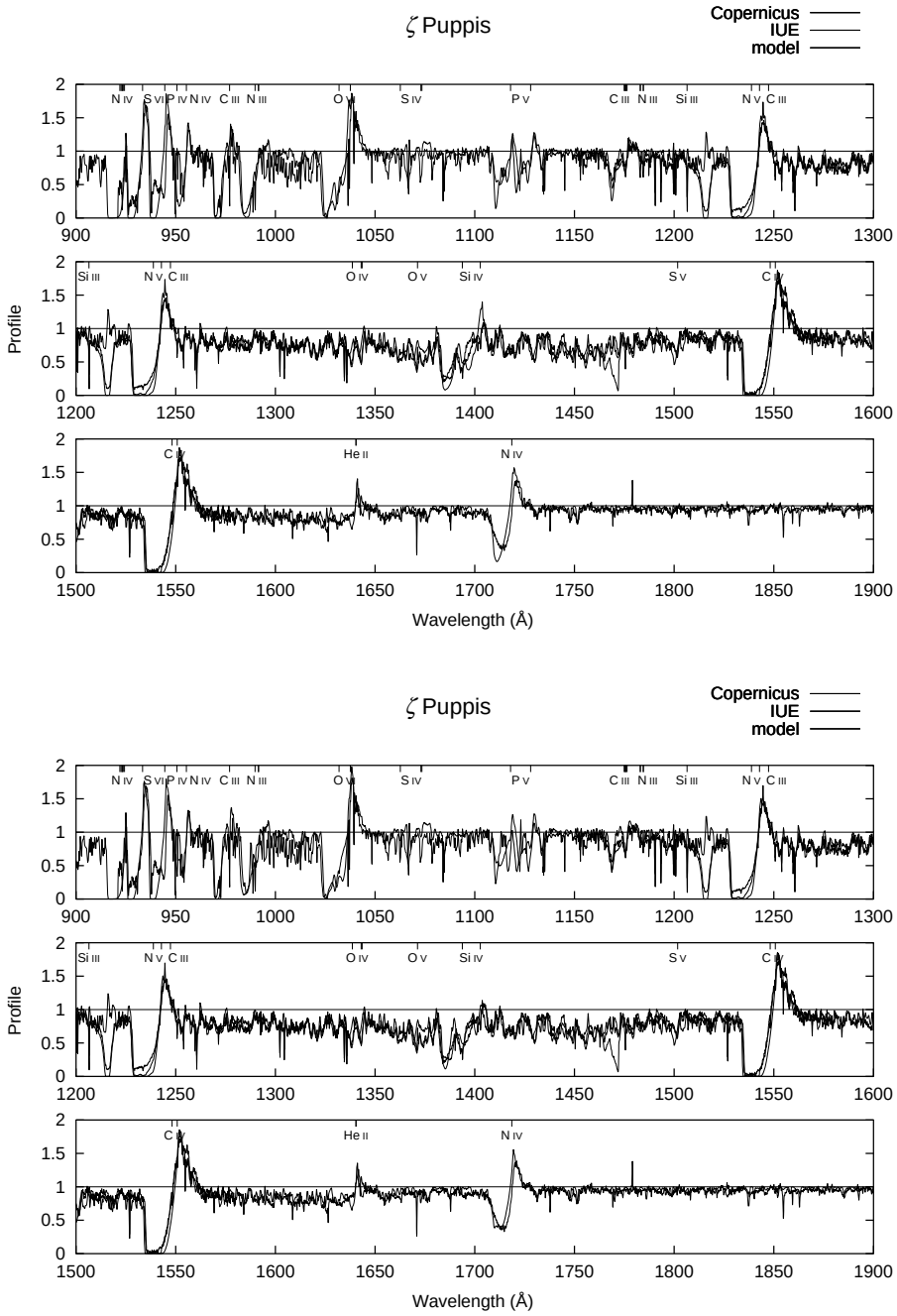

Figure 19: Calculated and observed UV spectrum for ζ Puppis. The observed spectrum shows the Copernicus and IUE high-resolution observations, and the calculated state-of-the-art spectra represent the final models of Pauldrach et al. 2003. For a discussion see text.

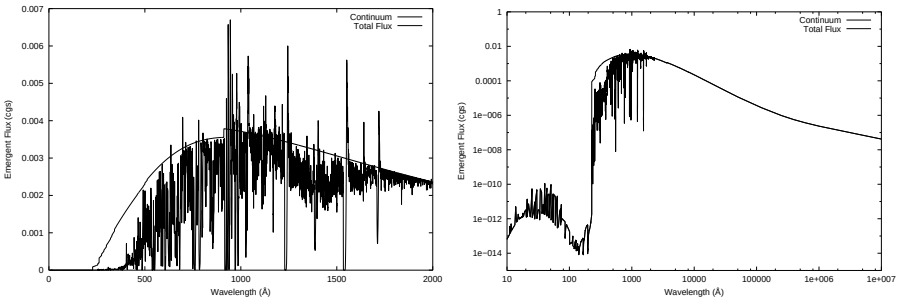

Figure 20: Calculated state-of-the-art spectral energy distribution of the final model of ζ Puppis of Pauldrach et al. 2003. *Left*: Linear scale for the flux. *Right*: Logarithmic scale for the flux.

and a simple treatment of emitted radiation from shock cooling zones. Thus, we conclude that a more consistent treatment of expanding atmospheres was still needed for a detailed analysis.

This more consistent treatment of expanding atmospheres that has now been applied and fixes the status quo is based on the improvements discussed in Section 6.1 (for a more comprehensive discussion see Pauldrach et al. 2001 and Pauldrach and Hoffmann 2003). As is shown in Figure 19, the calculated synthetic spectrum is quite well in agreement with the spectra observed by IUE and Copernicus. The small differences observed in the Si IV and the N IV lines just reflect a sensitive dependence on the parameters used to describe the shock distribution. This is verified by a comparison of the two panels of Figure 19, where just the shock-distribution has slightly been changed within the range of uncertainty of the corresponding parameters. Not only have the stellar and wind parameters of this object been confirmed by the model on which the synthetic spectrum is based, but also the abundances of C, N, O, P, Si, S, Fe, and Ni have been determined. We thus conclude that the present method of quantitative spectral UV analysis of Hot Stars leads to models which can be regarded as being realistic.

Consequently, we consider these kind of quantitative spectral UV analyses as the ultimate test for the accuracy and the quality of theoretical ionizing fluxes (cf. Figure 20), which can thus be used as spectral energy distributions for the analysis of H II regions.

7.2.2 UV Analysis of the Cool O Supergiant α Cam

In Figure 21 it can be seen that the method also works for cool O supergiants like α Cam. We recognize again that the synthetic spectrum is quite well in agreement with the IUE and Copernicus spectra (for a discussion see Pauldrach et al. 2001). In the uppermost panel of the spectrum, simulations of interstellar lines have additionally been merged with the synthetic spectrum in order to disentangle wind lines from interstellar lines (for a discussion of this point see Hoffmann 2002). In this case also, our new realistic models allowed to determine stellar parameters, wind parameters, and abundances from the UV spectra alone. (The operational procedure of the

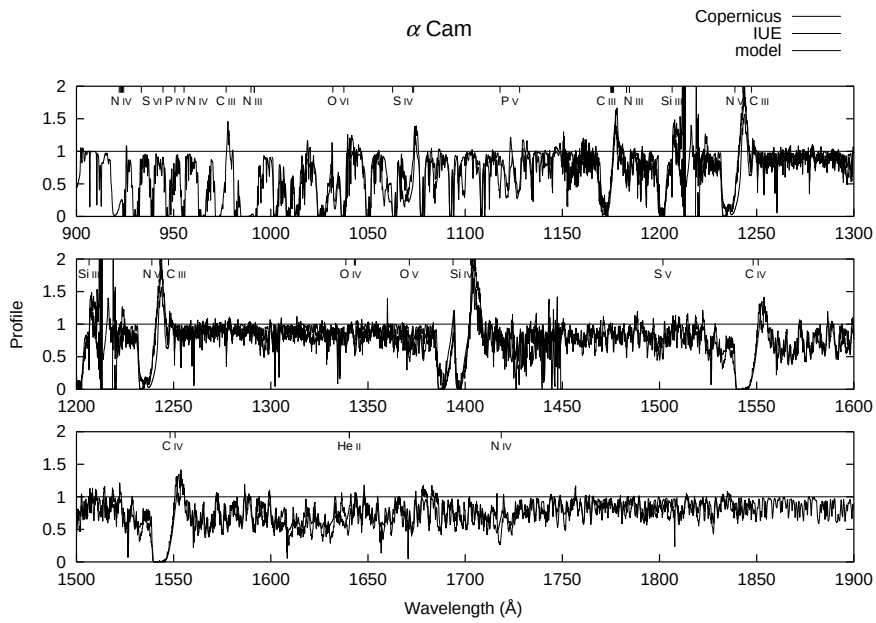

Figure 21: Comparison of the best model of Pauldrach et al. 2001 with spectra of α Cam observed by IUE and Copernicus, demonstrating the quality that can be achieved with the new model generation.

method begins with realistic estimates of R, $T_{\rm eff}$, M, and a set of abundances. With these, the model atmosphere is solved and the velocity field, the mass loss rate $\dot{M}$, and the synthetic spectrum is calculated. The parameters are adjusted and the process is repeated until a good fit to all features in the observed UV spectrum is obtained. For a compact description of this procedure see Pauldrach et al. 2002). It turned out that the effective temperature can be determined to within a range of ± 1000 K and the abundances to at least within a factor of 2.

7.3 Wind properties of massive O stars

As a last point we want to illustrate the significance of the dynamical parameters of radiation-driven winds. The intrinsic significance is quite obvious: it is the consistent hydrodynamics which provides the link between the stellar parameters ($T_{\rm eff}$, M, R) and the wind parameters (v_∞, $\dot{M}$). Thus, the appearance of the UV spectrum is determined by the interplay of the NLTE model and the hydrodynamics. (As was discussed in Section 6.1, the hydrodynamics is controlled by the line force, which is primarily determined by the occupation numbers, and the radiative transfer of the NLTE model, but the hydrodynamics in turn affects the NLTE model via the density and velocity structure.)

A tool for illustrating the significance of the dynamical parameters is offered by the so called *wind-momentum–luminosity relation*. This relation is based on two important facts: The first one is that, due to the driving mechanism of hot stars,

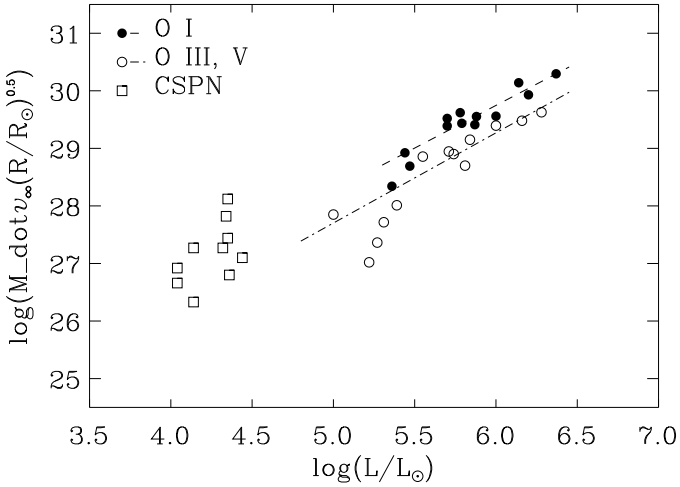

Figure 22: The wind-momentum–luminosity relation for massive O stars and Central Stars of Planetary Nebulae (CSPNs). Circles designate the O star analysis based on Hα profiles by Puls et al. 1996, and squares that of CSPNs by Kudritzki et al. 1997. Figure from Kudritzki and Puls 2000.

the mechanical momentum of the wind flow ($v_\infty \dot{M}$) is mostly a function of photon momentum (L/c) and is therefore related to the luminosity. The second one is that the expression $v_\infty \dot{M} R^{1/2}$ is an almost directly observable quantity. As the shapes of the spectral lines are characterized by the strength and the velocity of the outflow, the first term of this expression, the observed terminal velocity, can be measured directly from the width of the absorption part of the saturated UV resonance lines. Deducing the mass-loss rate from the line profiles is, however, more complex, since this requires the calculation of the ionization balance in advance. On the other hand, the advantage is that optical lines like Hα can be used for this purpose. Thus, the product of the last two terms of the expression $v_\infty \dot{M} R^{1/2}$ directly follows from a line fit of Hα (cf. Puls et al. 1996). The dynamical parameters obtained in this way are usually designated as *observed wind parameters*. Figure 22 shows that the wind-momentum–luminosity relation indeed exists for massive O stars, as they follow the linear relation predicted by the theory, in a first approximation and for fixed metallicities. With regard to the spread in wind momenta found by Kudritzki et al. (1997) for the Central Stars of Planetary Nebulae (lower part of Figure 22), Pauldrach et al. (2002, 2003) have given a solution which, however, is unlikely to be believed yet by the part of the community working on stellar evolution.

Moreover, it is important to note that as a by-product of this relation it can be used as an independent tool for measuring extragalactic distances up to Virgo and Fornax, since it is independent of the observationally unknown masses (for a recent and comprehensive review on this subject see Kudritzki and Puls 2000).

Figure 23 shows that the observed behavior of the wind momentum luminosity relation is represented quite well by our improved realistic models, particularly in the case of the two supergiants (ζ Puppis and α Cam) analyzed in Section 7.2. But,

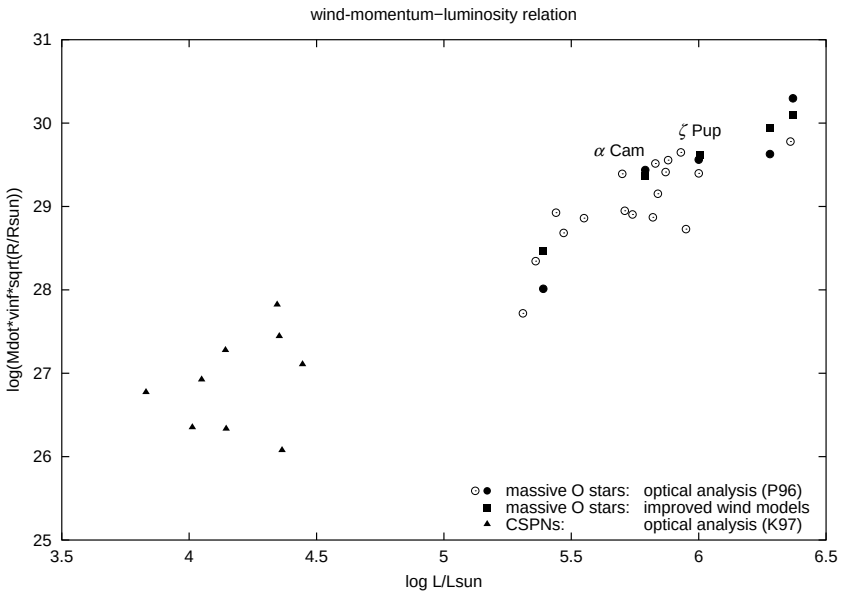

Figure 23: The wind-momentum–luminosity relation for massive O stars and CSPNs as in Figure 22. Also plotted as filled squares are the calculated wind momenta for five massive O stars; filled circles designate the corresponding observed values (cf. Pauldrach et al. 2002, 2003).

as already pointed out, this relation is independent of the stellar mass. Thus, in order to verify the statement of the previous section that the observed stellar and wind parameters are confirmed by the present models, we also have to investigate the relations of the individual dynamical parameters.

For this investigation we need to use as input for our models the same stellar parameters as have been used to obtain the observed wind parameters. On the basis of this requirement, Figure 24 (upper panel) shows that the observed and predicted values of the terminal velocities (v_∞) are in agreement to within 10 %. Since v_∞ is proportional to the escape velocity ($v_{\rm esc}$)

$$v_\infty \propto v_{\rm esc} = \left(\frac{2GM}{R}(1-\Gamma)\right)^{1/2}$$

which strongly depends on the mass of the objects, *the mass is determined very accurately by the predicted values* (G is the gravitational constant and Γ is the ratio of radiative Thomson acceleration to gravitational acceleration). For the mass-loss rates we found agreement to within a factor of two, as shown in Figure 24 (lower panel). Due to the strong relation between the mass-loss rates and the luminosities ($\dot{M} \propto L$), *the luminosities can thus be precisely determined*.

Therefore, computing the wind dynamics consistently with the NLTE model permits not only the determination of the wind parameters from given stellar parameters,

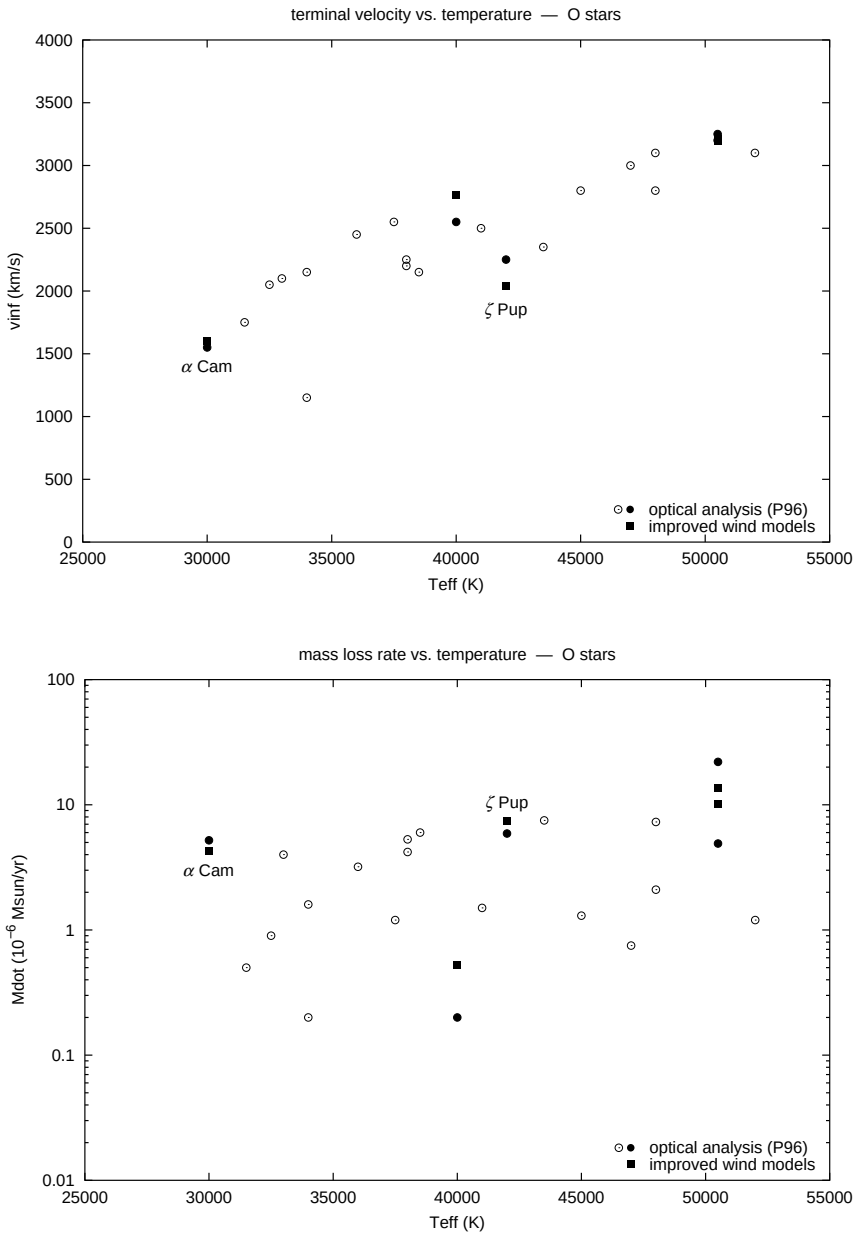

Figure 24: *Top*: Terminal velocities as a function of effective temperature for massive O-stars of the same sample as in Figure 23. *Bottom*: Mass-loss rates as a function of effective temperature for the same sample. The calculated values for the five massive O stars are designated by filled squares; filled circles designate the corresponding observed values (cf. Pauldrach and Hoffmann 2003 concerning ζ Puppis; the other objects have been treated by Hoffmann and Pauldrach 2002).

but conversely makes it possible *to obtain the stellar parameters from the observed UV spectrum alone*. As stated above, this means that, in principle, *the stellar parameters can immediately be read off by simply comparing an observed UV spectrum to a proper synthetic spectrum*. However, the whole procedure is not always an easy task, since in most cases a comprehensive grid of models and some experience will be required to do so. Although the idea itself is not new (cf. Pauldrach et al. 1988 and Kudritzki et al. 1992), only the new generation of models has reached the degree of sophistication that makes such a procedure practicable instead of purely academic. The corresponding conclusion is that *realistic models are characterized by at least a quantitative spectral UV analysis calculated together with a consistent dynamics*.

8 Conclusions and Outlook

The **need** for **detailed atmospheric models** of **Hot Stars** has been motivated in depth and a **diagnostic tool** with great astrophysical potential has been presented.

It has been shown that the models of the *new generation* are realistic. They are *realistic* with regard to a *quantitative spectral UV analysis* calculated, for the case of O stars, along with consistent dynamics, which, in principle, allows to read off the stellar parameters by comparing an observed UV spectrum to a suitable synthetic spectrum. The new generation of models has reached a degree of sophistication that makes such a procedure practicable.

The astronomical perspectives are enormous. Of course, there is still a large amount of hard and careful astronomical work that needs to be done. The diagnostic tool for expanding model atmospheres is in our hands, but this is (as usual) just the starting point; further elaboration, refinements, and modifications are required before the results are quantitatively completely reliable.

But this is not the handicap for the future. The present handicap are future observations. What is most urgently needed is the **Next Generation Space Telescope**.

With respect to the topics discussed in this review this telescope is needed for a variety of reasons:

To tackle the question whether **Supernovae Ia** are standard candles in a cosmological sense realistic models and synthetic spectra of Type Ia Supernovae require *spectral observations of objects at mid-redshift* and sufficient resolution. The context of this question is the current surprising result that distant SNe Ia at intermediate redshift appear fainter than standard candles in an empty Friedmann model. Consequently, the current SN-luminosity distances indicate an accelerated expansion of the universe.

In order to be able to make quantitative predictions about the influence of very massive, extremely metal-poor **Population III** stars on their galactic and intergalactic environment one primarily needs observations which can be compared to the predicted flux spectra that are already available for zero metallicity and can, in principle, be produced for metallicities different from zero. Observations with the Next Generation Space Telescope (NGST) of distant stellar populations at high redshifts will give us the opportunity to deduce the primordial IMF, thus allowing a quantitative

investigation of the ionization efficiency of a Top-heavy IMF via *realistic spectral energy distributions* of these very massive stars.

NGST observations are also important for determining extragalactic abundances and population histories of **starburst galaxies** from an analysis of H II regions. This task also requires energy distributions of time-evolving stellar clusters, which are calculated on the basis of a grid of *spectral energy distributions* of O and early B-type stars. A crucial point with respect to this is whether the spectral energy distributions of massive stars are already realistic enough to be used for diagnostic issues of H II regions. It has been shown in this review that the *ultimate test* is provided by a comparison of observed and synthetic UV spectra of individual massive stars, since the ionization balance can be traced reliably through the strength and structure of the wind lines formed throughout the atmosphere.

Furthermore, NGST is important for directly exploiting the diagnostic perspectives of galaxies with pronounced current star formation. It has been demonstrated that massive stars dominate the UV wavelength range in **star-forming galaxies**, and that therefore the UV-spectral features of massive O stars can be used as tracers of age and chemical composition of starburst galaxies even at high redshift. This is in particular the case when the flux from these galaxies is amplified by gravitational lensing through foreground galaxy clusters; corresponding observations render the possibility of determining metallicities of starbursting galaxies in the early universe via *realistic UV spectra* (in the rest frame) of massive O stars.

As a final remark it is noted that the solution method of stationary models for expanding atmospheres is in its present stage already regarded as a standard procedure towards a realistic description. Thus, together with an easy-to-use interface and an installation wizard, the program package **WM-basic** has been made available to the community and can be downloaded from the author's home page.

Acknowledgments

I wish to thank my colleagues Tadziu Hoffmann and Tamara Repolust for proofreading the manuscript, and I am grateful to Amiel Sternberg and Claus Leitherer for providing me with figures from their publications. This research was supported by the Sonderforschungsbereich 375 of the Deutsche Forschungsgemeinschaft, and by the German-Israeli Foundation under grant I-551-186.07/97.

References

Baldwin, J.A., Ferland, G.J., Martin, P.G. et al. 1991, ApJ 374, 580

Bromm, V., Coppi, P.S., Larson, R.B. 1999, ApJ 527, L5

Bromm, V., Kudritzki, R.P., Loeb, A. 2001, ApJ 552, 464

Carr, B.J., Bond, J.R., Arnett, W.D. 1984, ApJ 277, 445

Cassinelli, J., Olson, G. 1979, ApJ 229, 304

Castor, J.I., Abbott, D.C., Klein, R. 1975, ApJ 195, 157

Conti, P.S., Leitherer, C., Vacca, W.D. 1996, ApJ 461, L87

El Eid, M.F., Fricke, K.J., Ober, W.W. 1983, A&A 119, 54

Fan, X. et al. 2000, AJ 120, 1167

Feldmeier, A., Kudritzki, R.-P., Palsa, R., Pauldrach, A. W. A., Puls, J. 1997, A&A 320, 899

Genzel, R. et al. 1998, ApJ 498, 579

Giveon, U., Sternberg, A., Lutz, D., Feuchtgruber, H., Pauldrach, A. W. A. 2002, ApJ 566, 880

Gunn, J.E., Peterson, B.A. 1965, ApJ 142, 1633

Hamann, W.R. 1980, A&A 84,342

Harnden, F.R., Branduardi, G., Elvis, M. et al. 1979, ApJ 234, L51

Hillebrandt, W., Niemeyer, J.C. 2000, ARA&A 38, 191

Hoffmann, T.L. 2002, Ph.D. thesis, LMU Munich

Hoffmann, T.L., Pauldrach, A.W.A. 2002, IAU Symposium 209, in press

Hummer, D.G., Rybicki, G.B. 1985, ApJ 293, 258

Kirshner, R.P., Jeffery, D.J., Leibundgut, B., et al. 1993, ApJ 415, 589

Kudritzki, R.P., Hummer, D.G., Pauldrach, A.W.A., et al. 1992, A&A 257, 655

Kudritzki, R.P., Méndez, R. H., Puls, J., McCarthy, J. K. 1997, in IAU Symp. 180, Planetary Nebulae, eds. H.J. Habing & H.J.G.L.M. Lamers, p. 64

Kudritzki, R.P., Puls, J. 2000, ARA&A 38, 613

Kudritzki, R.P. 2002, ApJ in press

Kunth, D., Mas-Hesse, J.M., Terlevich, R., et al. 1998, A&A 334, 11

Kurucz, R.L. 1992, Rev. Mex. Astron. Astrof. 23, 181

Lamers, H.J.G.L.M., Morton, D.C. 1976, ApJ Suppl. 32, 715

Larson, R.B. 1998, MNRAS 301, 569

Leibundgut, B. 2001, ARA&A 39, 67

Leitherer, C., Leão, J., Heckman, T.M., Lennon, D.J., Pettini, M., Robert, C. 2001, ApJ 550, 724

Lucy, L.B., Solomon, P. 1970, ApJ 159, 879

Lucy, L.B., White, R. 1980, ApJ 241, 300

Lutz, D. et al. 1996, A&A 315, 137

Loeb, A. 1998, in ASP Conf. Ser. 133, 73

Milne, E.A. 1926, MNRAS 86, 459

Morton, D.C., Underhill, A.B. 1977, ApJ Suppl. 33, 83

Nomoto, K., Thielemann, F.-K., Yokoi, K. 1984, ApJ 286, 644

Nugent, P., Baron, E., Branch, D., et al. 1997, ApJ 485, 812

Oey, M.S., Massey, P. 1995, ApJ 452, 210

Owocki, S., Castor, J., Rybicki, G. 1988, ApJ 335, 914

Pauldrach, A.W.A., Puls, J., Kudritzki, R.P. 1986, A&A 164, 86

Pauldrach, A.W.A. 1987, A&A 183, 295

Pauldrach, A.W.A., Herrero, A. 1988, A&A 199, 262

Pauldrach, A.W.A., Puls, J., Kudritzki R.-P., et al. 1988, A&A 207, 123

Pauldrach, A.W.A., Feldmeier, A., Puls, J., Kudritzki, R.-P. 1994b, in Space Sci. Rev. 66, 105

Pauldrach, A.W.A., Kudritzki, R.-P., Puls, J., et al. 1994, A&A 283, 525

Pauldrach, A.W.A., Duschinger, M., Mazzali, P.A., et al. 1996, A&A 312, 525

Pauldrach, A.W.A., Lennon, M., Hoffmann, T.L., et al. 1998, in: Proc. 2nd Boulder-Munich Workshop, PASPC 131, 258

Pauldrach, A.W.A., Hoffmann, T.L., Lennon, M. 2001, A&A 375, 161

Pauldrach, A.W.A., Hoffmann, T.L., Mendez, R.H. 2002, IAU Symposium 209, in press

Pauldrach, A.W.A., Hoffmann, T.L., Mendez, R.H. 2003, A&A, in press

Pauldrach, A.W.A., Hoffmann, T.L. 2003, A&A, in press

Perlmutter, S., Aldering, G., Goldhaber, G., et al. 1999, ApJ 517, 565

Pettini, M., Kellogg, M., Steidel, C.C., et al. 1998, ApJ 508, 539

Pettini, M., Steidel, C.C., Adelberger, K.L., Dickinson, M., Giavalisco, M. 2000, ApJ 528, 96

Puls, J. 1987, A&A 184, 227

Puls, J., Pauldrach, A.W.A. 1990, PASPC 7, 203

Puls, J., Kudritzki R.-P., Herrero A., Pauldrach, A.W.A., Haser, S.M., et al. 1996, A&A 305, 171

Reinecke, M., Hillebrandt, W., Niemeyer, J.C. 1999, A&A 374, 739

Riess, A.G., Filippenko, A.V., Challis, P., et al. 1998. Astron. J. 116, 1009

Riess, A.G., Kirshner, R.P., Schmidt, B.P., et al. 1999, Astron. J. 117, 707

Rybicki, G.B. 1971, JQSRT 11, 589

Rubin, R.H., Simpson, J.P., Haas, M.R., et al. 1991, PASP 103, 834

Saha, A., Sandage, A., Thim, F., Labhardt, L., Tammann, G.A., Christensen, L., Panagia, N., Macchetto, F. 2001, ApJ, 551, 973

Sauer, D., Pauldrach, A.W.A. 2002, Nucl. Astrophys., MPA/P13

Seward, F.D., Forman, W.R., Giacconi, R., et al. 1979, ApJ 234, L55

Schaerer, D., de Koter, A. 1997, A&A 322, 598

Sellmaier, F.H., Yamamoto, T., Pauldrach, A.W.A., Rubin, R.H. 1996, A&A, 305, L37

Simpson, J.P., Colgan, S.W.J., Rubin, R.H., et al. 1995, ApJ 444, 721

Sobolev, V. 1957, Sov. A&A J. 1, 678

Steidel, C.C., Giavalisco, M., Pettini, M., Dickinson, M., Adelberger, K.L. 1996, ApJ 462, L17

Sternberg, A., Hoffmann, T.L., Pauldrach A.W.A. 2002, ApJ, in press

Thornley, M.D., Förster-Schreiber, N.M., Lutz, D., et al. 2000, ApJ 539, 641

Walborn, N.R., Nichols-Bohlin, J., Panek, R.J. 1985, IUE Atlas of O-Type Spectra from 1200 to 1900Å (NASA RP-1155)